Upshot of generalized Fourier's and Fick's laws on MHD Williamson nanofluid flow past a bi-directional stretched surface with second order slip and double stratification

Thesis Submitted By

ASMA LIAQUET
(01-248172-002)

Supervised By

Prof. Dr. M. Ramzan

A dissertation submitted to the Department of Computer Science, Bahria University, Islamabad as a partial fulfilment of the requirements for the award of the degree of MS

Session (2017 - 2019)

Bahria University
Discovering Knowledge

MS-13

Thesis Completion Certificate

Scholar's Name: **Asma Liaquet** Registration No. **01-248172-002**

Programmed of Study: **MS (Mathematics)**

Thesis Title: **"Upshot of generalized Fourier's and Fick's laws on MHD Williamson nanofluid flow past a bi-directional stretched surface with second order slip and double stratification"**

It is to certify that the above student's thesis has been completed to my satisfaction and, to my belief, its standard is appropriate for submission for Evaluation. I have also conducted plagiarism test of this thesis using HEC prescribed software and found similarity index at 11 % that is within the permissible limit set by the HEC for the MS/MPhil degree thesis.

I have also found the thesis in a format recognized by the BU for the MS/MPhil thesis.

Principal Supervisor's Signature: _____ 20/06/2019

Date: 20/06/2019 **Name:** **Dr. Muhammad Ramzan**

Dedicated to

My beloved husband, my parents, my in laws, my brothers,
sisters and respected teachers

whose prayers and support have always been a source of inspiration

and encouragement for me.

My caring and supporting husband and lovely son

have always given me care and love.

Acknowledgments

I am thankful to Almighty ALLAH Who has enabled me to learn and to achieve milestones towards my destination and His beloved Prophet Hazrat Muhammad (ﷺ) Who is forever a constant source of guidance, a source of knowledge and blessing for entire creation. His teachings show us a way to live with dignity, stand with honour and learn to be humble.

My acknowledgment is to my kind, diligent and highly zealous supervisor, Prof. Dr. M. Ramzan, who supported me with his cherished opinions and inspirational discussions. His valuable expertise, comments, suggestions and instructions are most welcome that greatly improved the clarity of this document. I am placing my earnest thanks to Prof. Dr. M. Ramzan. I am so grateful to work under the supervision of such a great person.

My gratitude is to my honorable professors who took me to the apex of my academia with their guidance. In particular, Dr. Rizwan ul haq and Dr. Jafar Hasnain who have always been supportive in all of my course work and kept encouraging me throughout the session in Bahria University, Islamabad Campus. They are the true teachers who have made Mathematics Department of BUIC, a real place of learning.

My intense recognition is to my in laws, mother, father, brothers, sisters and husband (for every thing) who are always real pillars for my encouragement and showered their everlasting love, care and support throughout my life. Humble prayers, continuing support and encouragement of my family are as always highly appreciated.

As usual, so many friends have helped me that I cannot list them all. Hina Gul, Habib Un Nisa, Nazia shameer, Sania Naseer were specially remained enormously helpful throughout the period of

my MS studies.

Consequently, My all plea is to Allah, the Almighty, the beneficent Whose blessings are always showered upon me via strengthening my wisdom and bestowed me with the knowledge of what he wants.

Asma Liaquet
Bahria University Islamabad, Pakistan
May 2019

Bahria University
Discovering Knowledge

MS-14A

Author's Declaration

I, **Asma Liaquet** hereby state that my MS thesis titled **"Upshot of generalized Fourier's and Fick's laws on MHD Williamson nanofluid flow past a bi-directional stretched surface with second order slip and double stratification"** is my own work and has not been submitted previously by me for taking any degree from this university **Bahria University Islamabad** or anywhere else in the country/world.

At any time if my statement is found to be incorrect even after my Graduate the university has the right to withdraw/cancel my MS degree.

Name of scholar: **Asma Liaquet**
Registration no: **53666**

Bahria University
Discovering Knowledge

MS-14B

Plagiarism Undertaking

I solemnly declare that research work presented in the thesis titled **"Upshot of generalized Fourier's and Fick's laws on MHD Williamson nanofluid flow past a bi-directional stretched surface with second order slip and double stratification "** is solely my research work with no significant contribution from any other person. Small contribution / help wherever taken has been duly acknowledged and that complete thesis has been written by me.

I understand the zero tolerance policy of the HEC and Bahria University towards plagiarism. Therefore I as an Author of the above titled thesis declare that no portion of my thesis has been plagiarized and any material used as reference is properly referred / cited.

I undertake that if I am found guilty of any formal plagiarism in the above titled thesis even after award of MS degree, the university reserves the right to withdraw / revoke my MS degree and that HEC and the University has the right to publish my name on the HEC / University website on which names of students are placed who submitted plagiarized thesis.

Student / Author's Sign: _____

Name of the Student: **Asma Liaquet**

Abstract:

In this proposed model, we have discussed the generalized Fick's and Fourier's laws over MHD Williamson nanofluid flow with mixed convection past a bidirectional stretched surface. Influence of variable thermal conductivity and stratification with second-order slip are also considered. Suitable transformations have betrothed to transform the partial differential equations into differential equations with high nonlinearity. The solution of the proposed problem has attained via some suitable analytical or numerical technique. Impacts of miscellaneous arising parameters have deliberated via graphical structures. Some useful tabulated values of physical quantities have also discussed.

List of Figures

List of tables

Nomenclature

u, v, w	Velocity components
μ	Viscosity
ρ	Density
η_1	Apparent viscosity
η	Similarity transformation variable
A_1	First Rivilin-Ericksen tensor
A_2	Second Rivilin-Ericksen tensor
τ_{yx}	Shear force
P	Pressure
k	Thermal conductivity
d / dt	Material time derivative
τ	Cauchy stress tensor
τ_w	Shear stress at wall
Pr	Prandtl number
γ^*	Biot number
c_p	Specific heat
D_e	Coefficient of mass diffusivity
k_n	Reaction rate of diffusivity species
T	Temperature

T_∞	Ambient temperature
T_0	Fluid reference temperature
C	Concentration
C_∞	Ambient concentration
C_0	Reference concentration of nano particles
D_B	Brownian diffusion coefficient
D_T	Thermophoretic diffusion coefficient
F	Homotopy
N	Non-linear operator
σ	Electrical conductivity
λ_C	Mass flux's relaxation time
k_0	Elastic parameter
λ_E	Heat flux's relaxation time
α_1	Normal stress moduli
ε	Thermal conductivity parameter
ν	Kinematic viscosity
λ^*	Second grade dimensionless parameter
γ_1^*	Heat transfer biot number
γ_2^*	Mass transfer biot number
M	Hartmann number

γ_1, γ_3	First order slip parameter
γ_2, γ_4	Second order slip parameter
β	Stretching ratio parameter
Nb	Brownian motion parameter
Nt	Thermophoresis parameter
δt	Thermal relaxation parameter
δc	Concentration relaxation parameter
Le	Lewis number
We	Williamson fluid parameter
Nr	Ratio of concentration to buoyancy forces
λ	Mixed convection parameter
Gr_x	Grashof number
Re_x	Local Reynold parameter
S_1	Thermal stratification parameter
S_2	concentration stratification parameter
β_2	Non-linear temperature's convection Parameter
β_3	Non-linear concentration's convection Parameter
C_{f_x}	Skin friction coefficients in x-direction
C_{f_y}	Skin friction coefficients in y-direction

Contents

Chapter 1

Introduction and Literature review

1.1 Introduction

The role of nanofluid is fundamental for the enhancement of thermal conductivity of conventional fluids. Nanofluids are vital in many engineering applications like in biomedical, engineering and many chemical processes. Nanofluid is composed of nano-meter sized particles (with diameter less than 100nm) and some traditional fluid. The nanoparticles are usually made of oxides, carbon nanotubes, metals or carbides. Ordinary fluids includes water, ethylene glycol and oil. Nanoparticle improves the thermophysical properties and heat transfer performance in many biological and industrial applications. Nanofluids are widely used in cooling of electronics, cooling of heat exchanging devices and improve their efficiency, automobile industry, in the solar collectors, in nuclear reactors and modern drug delivery system. Nanoparticles effect the heat and mass transfer characteristics. Thermal conductivity and convected heat transfer in nanofluids are greater when compared with the traditional fluid. Nanofluids have an remarkable combination of four characteristic properties intended in thermal and fluid systems:

- At low nanoparticle concentrations thermal conductivity is enhanced.
- Strong temperature dependent thermal conductivity.
- Non-linear enhancement in thermal conductivity with nanoparticle concentration.
- Increasing in boiling critical heat flux.

Magneto hydro dynamic (MHD) principle is applied for generating power from coal fired or reactor power plants. MHD generator plant does not require any turbine any turbine and does not have any generator shaft. In a MHD generator the thermal energy in plasma (hot ionized gas) is directly converted to electrical energy (without intermediate conversion to mechanical shaft energy). When an electric conductor moves across a magnetic field, a voltage is induced in it which produces an electric current. In MHD generator, the solid conductors are replaced by a gaseous conductor, an iodized gas. If such a gas is passed at a high velocity through a powerful magnetic field, a current is generated and can be extracted by placing electrodes in suitable position in the stream.Fourier's coined work was considered to be the most effective model that has been used as a benchmark for decades because of its wideranging applications. One of the shortcomings of this model was that it often leads to a parabolic energy equation which specifies that initial disturbance was immediately encountered by the medium under consideration. Anomaly in the Fourier's law named as "Paradox in heat conduction" was addressed by Cattaneo by insertion of relaxation time. It is witnessed that this modification produces the hyperbolic energy equation and enable the transport of heat by means of propagation of thermal waves with limited speed. Later on, Christov upgraded Cattaneo's model by replacing the Oldroyd upperconvected derivative for time derivative. This improved version is now-a-days termed as the Cattaneo–Christov heat flux model. Fick's law states that the rate of diffusion of a gas into the liquid is:

Directly proportional to:

- the partial pressure of the gas above the liquid
- surface area of avaible for gas exchange
- solubility co-efficient of the gas

Inversely proportional to

- Gram molecular weight of the molecules
- Thickness of the membrane

Sometimes the mechanism of deformable density happened/appeared in the shallow fluid medium owing to change in the state of concentration, pressure, temperature and dissolved

substances termed as stratification. It is witnessed that in case of stratification, density is the function of space variable as well as time. By cause of which layer formation occurs. Newton's law of viscosity states that shear stress is directly proportional to the velocity gradient but in a linear manner. Non-Newtonians fluids are those fluids which do not obey Newton's law of viscosity. In these fluids shear force and velocity gradient are directly propotional but in non-linear manner. Here, the viscosity is non-uniform under the shear force. Williamson fluid symbolizes as a non-Newtonian fluid along with shear thinning property (*i.e.* viscosity tends to decrease when shear stress increases). The flows in which the fluid is forcefully directed over a surface and the effect of buoyancy force are also significant, such flows are named as mixed convection flows. An example of this would be a fan blowing upward on a heated plate. It is also define as, combined forced convection and natural convection, or mixed convection, occurs when natural convection and forced convection mechanisms act together to transfer heat. This is also defined as situations where both pressure forces and buoyant forces interact.

1.2 Literature Review

Heat transfer phenomenon plays a vital role when the temperature varies between different bodies or parts of the same body. Heat can be transferred by three methods: convection of fluids, conduction in solids and by radiation. To examine body heat transfer, the principle of heat transfer can be enforced to the human body. Here, we can quote one example i.e., the metal pan is used to transfer heat from the stove to food. Some applications of heat transfer are: cooking food over metal pots, boiling milk in metal pots and thermal treatment of pain by hot water bag. Straughan [1] considered the Cattaneo-Christov heat flux model for the consideration of thermal convection over a Newtonian fluid. Khan et al. [2] analyzed numerically by engaging bvp4c MATLAB based function the flow of Sisko fluid flow accompanied generalized Fick's and Fourier's laws over a nonlinear stretched surface. Hayat et al. [3] examined analytically the MHD flow of Jeffrey fluid past a variable thick surface with impacts of the chemical reaction and Cattaneo-Christov heat flux in a stratified medium. Waqas et al. [4] investigated that on the contrary of conventional Fourier's law of heat conduction; the energy equations innovated by employing Cattaneo-Christov heat flux model. It was observed that variable thermal

conductivity is in inverse proportionate to a temperature profile. The Soret Dufour effect on the flow of second-grade fluid between inclined parallel walls was analyzed by Khan et al. [5]. Ghadikolaei et al. [6] discussed the heat transfer characteristics of the incompressible flow of second-grade fluid generated by a stretching sheet. The dual behavior of viscosity was observed for both velocity and temperature. The influence of homogenous–heterogeneous reactions on heat transfer flow due to a stretching sheet was examined by Khan et al. [7]. They noticed that homogenous–heterogeneous reactions reduce fluid concentration.

In modern engineering processes especially in metallurgical engineering and metal working practices, the role of magnetohydrodynamics (MHD) is fundamental in the case of electrically conducting fluids. The function of the magnetic field is crucial in cooling the hot plasma inside a nuclear reactor vessel. Similarly, the magnetic field employed for the mixing of metals inside an electrical furnace [8]. Chamkha and Al-Mudhaf [9] demonstrated the effect of magnetic field on unsteady mixed convection flow past a cone rotating in an ambient fluid with a time-dependent angular velocity in. Later, free convection flow over a non-isothermal vertical cone with variable surface temperature was analyzed by Pullepu et al. [10]. Akbar et al. [11] investigated the two dimensional electrically conducting the flow of hyperbolic tangent fluid over a stretching surface. They observed that the increase in Hartmann number reduces fluid velocity in the vicinity of the stretching sheet. Seini and Makinde [12] illustrated the magnetic effects in stagnation point flow due to stretching surface in the presence of velocity slip. They perceived that the influence of magnetic field on velocity profile is more significant. On the other hand, the effect of transverse magnetic field on unsteady mixed convection flow over a porous cone in the presence of chemical reaction and heat generation/absorption was presented by Ravindran et al. [13]. Boland et al. [14] simulated MHD flow of viscous fluid over a circular cylinder wrapped with a permeable layer. They adopted the Darcy-Brinkman-Forchheimer model to study the flow inside the porous medium. Ellahi et al. [15] investigated the impact of Hall current on MHD Jeffrey fluid flow through a non-uniform duct. Mishra et al. [16] explored the heat mas transfer flow of viscoelastic fluid in the presence of a magnetic field. They concluded that the effect of magnetic field on velocity profile is opposite to temperature and concentration profiles. Further, the physical and computational aspects of the applied magnetic field on non-Newtonian fluid flow over a stretching surface was studied by Hussain et al. [17].

The role of nanofluid is fundamental for the enhancement of thermal conductivity of conventional fluids. Nanofluids are vital in many engineering applications like in biomedical, engineering and many chemical processes. Nanofluid is composed of nano-meter sized particles with diameter less than 100nm and some traditional fluid. The basic aim of using nanofluids in the traditional fluid is to enhance the thermal conductivity and improving heat transfer capability so as to attain better cooling. Khan and Pop [18] analyzed nanofluid flow over a stretching sheet. Makinde and Aziz [19] extended the work of Khan and Pop [18] and investigated the nanofluid flow in the presence of convective boundary condition. Nadeem et al. [20] studied the non-orthogonal stagnation point flow of a second-grade nanofluid towards the stretching surface. The influence of variable magnetic field on the nanofluid flow between two disks was explored by Hatami et al. [21]. They found the analytical solution via Homotopy perturbation method and noticed that the temperature boundary layer thickness reduces with the increase of Brownian motion parameter and thermophoretic parameter. The flow of a nanofluid in a permeable medium over a convectively heated permeable shrinking sheet is examined by Hayat et al. [22]. Sheikholeslami et al. [23] and Sheikholeslami and Rokhni [24] deliberated the influence of magnetic field on forced and free convection flow of nanofluids respectively by using the two-phase model. Hassan et al. [25] elaborated convective transport of heat transfer in a nanofluid through a porous medium. They concluded that convection heat transfer is improved by nanoparticles concentration. magnetic field effects on second order slip flow. Nayak et al. [26] focused on the numerical solution of the 3D nanofluid flow with nonlinear thermal radiation with slip and convective conditions. Hosseini et al. [27] studied the MHD flow of a nanofluid in a micro-channel heat sink via KKL model. They noticed that the interaction between nanoparticles and solid phase enhanced the Nusselt number. In recent years, several scientists have used nanofluid heat transfer in their studies [28-34] and many therein.

The aforementioned literature review discloses that three-dimensional MHD flow of Williamson nanofluid over a bi-directional stretched surface in the presence of second-order slip and double stratification is still scarce. The governing equations are transformed using similarity transformations and the solved analytically via Homotopy analysis method (HAM). The effects of pertinent parameters are displayed graphically and discussed.

Chapter 2

Basic preliminaries and laws

This chapter includes some important essential definitions, concepts and laws that are favorable in realizing the concepts in the second and third chapters.

2.1 Fluid

Fluid is a material which changes continuously when shear force is employed. For example, liquids and gases.

2.1.1 Liquid

Fluid having specific volume but no specific shape is known as liquid. Blood, water and milk etc, are the examples of liquid.

2.1.2 Gas

It is the type of fluid that has no specific volume and specific shape. For example, oxygen, hydrogen and nitrogen etc.

2.2 Fluid mechanics

The branch of physical sciences which deal with the fluid's behavior at rest or in motion. It has following two subclasses:

2.2.1 Fluid statics

It associates fluid's properties that are at rest.

2.2.2 Fluid dynamics

This represents the properties of fluids that are in motion.

2.3 Stress

Stress is the surface force applying upon the unit area along with the deformable body. It's unit in SI system is Nms^{-2} or $\frac{kg}{ms^2}$ and dimension is M/LT^2. It is classified into two types.

2.3.1 Shear stress

When force is applied parallel to the unit area of the surface then the stress is termed as shear stress.

2.3.2 Normal stress

Stress is known as normal stress when force is applied normal to the surface of unit area.

2.4 Strain

When a force is applied on an object,the substance used to compute its deformation termed as strain.

2.5 Flow

Flow is expressed as a substance that deforms smoothly and continuously under the impacts of various type of forces. It has following two catagories:

2.5.1 Laminar flow

When fluid flows in such a way that various fluid's layers do not cross each other and at every point velocity is taken constant is termed as laminar flow.

2.5.2 Turbulent flow

When fluid flows in such a way that various fluid's layers cross each other and velocity varies at every point with both direction and magnitude named as turbulent flow.

2.6 Viscosity

It is the essential fluid property which computes the resistance of fluid contrary to any gradual deformation when various forces are acting on it. Following are two ways that expresses the viscosity:

2.6.1 Dynamic viscosity

The characteristic of fluid that measures the fluid resistance against any deformation when a force acts on it. Numerically, it can be defined as:

$$\text{viscosity } (\mu) = \text{shear stress/gradient of velocity.} \tag{2.1}$$

SI units of viscosity are Ns/m^2 and it's dimension is $[M/LT]$.

2.6.2 Kinematic viscosity

It expresses the ratio of the dynamic viscosity (μ) to the fluid's density (ρ) . Numerically, it is given by:

$$\frac{\mu}{\rho}. \tag{2.2}$$

Its SI unit is $\frac{m^2}{s}$ and its dimension is $\left[L^2/T\right]$.

2.7 Newton's law of viscosity

It states that shear stress is directly proportional to the velocity gradient but in a linear manner. Numerically, it is represented as:

$$\tau_{yx} \propto du/dy, \tag{2.3}$$

or

$$\tau_{yx} = \mu_1 \left(du/dy \right), \tag{2.4}$$

where τ_{yx} describes the shear force acting on the fluid's element and μ_1 stands for the proportionality constant.

2.7.1 Newtonian fluids

Fluids which obey the Newton's law of viscosity are known as Newtonian fluids and the viscosity is uniform under the shear force. Here shear force and velocity gradient are linearly and directly propotional. For example air, water, glycerine, milk, mineral, and kerosene oil.

2.7.2 non-Newtonian fluids

Non-Newtonians fluids are those fluids which do not obey Newton's law of viscosity. In these fluids shear force and velocity gradient are directly propotional but in non-linear manner. Here, the viscosity is non-uniform under the shear force. Numerically, it is given by:

$$\boldsymbol{\tau}_{yx} \propto \left(du/dy \right)^n, \ n \neq 1, \tag{2.5}$$

or

$$\boldsymbol{\tau}_{yx} = \eta_1 (du/dy) \qquad ; \ \eta_1 = k \left(du/dy \right)^{n-1}, \tag{2.6}$$

in which η_1, n and k describes the apparent viscosity, flow behavior's index and consistency index respectively. For $n = 1$, Eq. (2.6) deforms to Newton's law of viscosity. Honey, paints and ketchup represents the non-Newtonian fluid behavior.

2.8 Second grade fluid

Abundant variety of fluids exists in nature.Thus some models of non-Newtonian fluids are discussed. The viscoelastic impacts of non-Newtonian fluids are generally characterized in three classes named as (i)differential, (ii)rate and (iii)integral types fluid.One important subclass of differential type fluid is second grade fluid. Second grade fluid describes the normal stress influences in between the neighbouring layers of fluid. Stress tensor discussed by Cauchy for

the viscous and second order fluids are defined as under:

$$\boldsymbol{\tau} = -p\mathbf{I} + \boldsymbol{\mu}\mathbf{A}_1, \quad \text{and} \quad \boldsymbol{\tau} = -p\mathbf{I} + \boldsymbol{\mu}\mathbf{A}_1 + \alpha_1\mathbf{A}_2 + \alpha_2\mathbf{A}_1^2, \tag{2.7}$$

where α_1 and α_2 represents the material constants respectively and $\mathbf{A}_1$ and $\mathbf{A}_2$ stands for the first and second Rivlin-Ericksen tensors. *i.e.*

$$\mathbf{A}_1 = (\text{grad}\mathbf{V}) + (\text{grad}\mathbf{V})^{\breve{\mathbf{T}}}, \tag{2.8}$$

$$\mathbf{A}_2 = d\mathbf{A}_1/dt + \mathbf{A}_1 (\text{grad}\mathbf{V}) + (\text{grad}\mathbf{V})^{\breve{\mathbf{T}}} \mathbf{A}_1. \tag{2.9}$$

The material moduli must satisfythe relations in the second order fluid case as:

$$\alpha_1 \leq 0, \ \mu \geq 0, \ \alpha_1 + \alpha_2 \neq 0. \tag{2.10}$$

The material moduli must fulfill the given relations for second grade fluid model as follows:

$$\alpha_1 \geq 0, \ \mu \geq 0, \ \alpha_1 + \alpha_2 = 0. \tag{2.11}$$

Using Cartesian coordinates we have

$$\text{grad}\mathbf{V} = \begin{bmatrix} u_x & u_y & u_z \\ v_x & v_y & v_z \\ w_x & w_y & w_z \end{bmatrix}, \quad (\text{grad}\mathbf{V})^{\breve{\mathbf{T}}} = \begin{bmatrix} u_x & v_x & w_x \\ u_y & v_y & w_y \\ u_z & v_z & w_z \end{bmatrix}. \tag{2.12}$$

2.8.1 Relaxation Time

When stress acts, a system deforms from equilibrium position to perturb position. After released stress, time is required for a perturb system back to equilibrium position is named as relaxation time.

2.9 Density

It is stated as the ratio of a mass of a substance to unit volume. This quantity is used to compute that how much stuff of a substance is present in the unit volume

Numerically it is expressed as:

$$\rho = \mu/\upsilon. \tag{2.13}$$

Its SI unit is $\frac{kg}{m^3}$.

2.10 Pressure

Pressure is expressed as a magnitude of force applied perpendicular to the surface per unit area. Numerically, it is represented by :

$$P = F/A. \tag{2.14}$$

Its SI unit is $\frac{N}{m^2}$.

2.11 Thermal conductivity

Thermal conductivity signifies energy transport through a body in the form of temperatue gradient. According to the second law of thermodynamics, heat flows in the direction of lower temperature.

Mathematically, it is expressed as:

$$\text{Thermal conductivity} = \frac{\text{heat flow x distance}}{\text{surface area x temperature difference}}.$$

Mathematically,

$$\kappa = Q_L/A(\Delta T), \tag{2.15}$$

where Q stands for quantity of heat, A stands for surface area and ΔT represents the change in temperature along distance L.

2.12 Convective boundary condition

Convective boundary condition generally states that heat flow over a surface through conduction is equal to the heat flow by convection and is termed as Robin boundary condition. Most general relation between the temperature of surface and surrounding is given through expression:

$$k\left(\partial T/\partial m_i\right)_{x_i} = h\left(T_f(x_i,t) - T_w(x_i,t)\right). \tag{2.16}$$

This equation shows that condition is equal to convection. In which h indentifies the heat transfer coefficient , x_i represents the coordinate at the boundary, T_f stands for the fluid's temperature and T_w stands for the wall temperature.

2.13 Nanofluid

The role of nanofluid is fundamental for the enhancement of thermal conductivity of conventional fluids. Nanofluids are vital in many engineering applications like in biomedical, engineering and many chemical processes. Nanofluid is composed of nano-meter sized particles (with diameter less than 100nm) and some traditional fluid. The nanoparticles are usually made of oxides, carbon nanotubes, metals or carbides. Ordinary fluids includes water, ethylene glycol and oil. Nanoparticle improves the thermophysical properties and heat transfer performance in many biological and industrial applications. Nanofluids are widely used in cooling of electronics, cooling of heat exchanging devices and improve their efficiency, automobile industry, in the solar collectors, in nuclear reactors and modern drug delivery system. Nanoparticles effect the heat and mass transfer characteristics. Thermal conductivity and convected heat transfer in nanofluids are greater when compared with the traditional fluid.

2.14 Williamsons Fluid

Williamson fluid symbolizes as a non-Newtonian fluid along with shear thinning property (*i.e.* viscosity tends to decrease when shear stress increases). An incompressible uni-directional flow of Williamson fluid along with pressure dependent viscosity in an inclined channel containing height h, is taken into account. We are assuming Cartesian coordinates system such that

$(u(y),0,0)$ is velocity vector where u represents velocity's x-component and y is perpendicular to x-axis. The equations which influence an incompressible fluid flow past a porous medium are given by:

$$\text{div } V = 0, \tag{2.17}$$

$$\rho \frac{dV}{dt} = \text{div } S, \tag{2.18}$$

in which ρ represents the density, S denotes the Cauchy stress tensor and d/dt be a sign of material time derivative.

The Cauchy stress tensor S for Williamson fluid is expressed as:

$$S = -pI + \tau, \tag{2.19}$$

$$\tau = \left(\mu_\infty + \frac{\mu_0 - \mu_\infty}{1 - \Gamma\dot{\gamma}}\right) \mathbf{A}, \tag{2.20}$$

in which τ stands for extra stress tensor, μ_0 and μ_∞ denote the limiting viscosity at zero and infinite shear rate, $\Gamma > 0$, shows time constant, A_1 signifies the first Rivilin Erickson tensor and $\dot{\gamma}$ is expressed as:

$$\dot{\gamma} = \sqrt{\frac{1}{2}\Pi}, \quad \Pi = \text{trace}(\mathbf{A}_1^2), \tag{2.21}$$

So,

$$\dot{\gamma} = (u_x)^2 + \frac{1}{2}(u_y + v_x)^2 + (v_y)^2, \tag{2.22}$$

where Π denotes the second invariant strain tensor, The case $\mu_\infty = 0$, taken into account and $\Gamma\dot{\gamma} < 1$, therefore with the help of given equation Eq.2.20, becomes

$$\tau = \left[\frac{\mu_0}{1 - \Gamma\dot{\gamma}}\right] \mathbf{A}_1,$$

with the help of Binomial expansion,we get

$$\tau = \mu_0[1 + \Gamma\dot{\gamma}]\mathbf{A}_1. \tag{2.23}$$

First Rivilin-Erickson tensor is expressed as

$$\mathbf{A}_1 = \begin{bmatrix} 2u_x & u_y + v_x \\ u_y + v_x & 2v_y \end{bmatrix}. \tag{2.24}$$

Cauchy stress tensor in component form is given by:

$$\begin{aligned} s_{xx} &= -p + 2\mu_0[1 + \Gamma\dot{\gamma}]u_x, \\ s_{yy} &= -p + 2\mu_0[1 + \Gamma\dot{\gamma}]u_y, \\ s_{xy} &= s_{yx} = -p + \mu_0[1 + \Gamma\dot{\gamma}](u_y + u_x), \\ s_{xz} &= s_{zx} = s_{zy} = s_{yz} = s_{zz} = 0. \end{aligned} \tag{2.25}$$

2.15 Magnetohydrodynamics

In modern engineering processes especially in metallurgical engineering and metal working practices, the role of magnetohydrodynamics (MHD) is fundamental in case of electrically conducting fluids. It is essentially derived from magneto (meaning magnetic field), hydro (meaning liquid) and dynamic(meaning movement of body by cause of forces). The function of magnetic field is crucial in cooling the hot plasma inside a nuclear reactor vessel. Similarly, magnetic field employed for the mixing of metals inside an electrical furnace. It can also be named as magnetofluiddynamics and hydromagnetics.

2.16 Mixed Convection

The flows in which the fluid is forcefully directed over a surface and the effect of buoyancy force are also significant, such flows are named as mixed convection flows. An example of this would be a fan blowing upward on a heated plate.

2.17 Modes of heat transfer

Heat transfer phenomenon plays a vital role when temperature takes different flows among the bodies. Basically, heat transports in three ways: convection, conduction and radiation. To examine body transfer heat, the principle of heat transfer can be enforced to the human body. Here, we can quote one example of metal pan that is used to transfer heat from the stove to food. Some applications of heat transfer are: cooking food over metal pots, boiling milk in metal pots and thermal treatment of pain by hot water bag.

2.17.1 Conduction

It is a technique in which heat transfer occurs from the more heated particles of a substance to the adjacent less heated particle as a result of contact between the material particles. Conduction is feasible in all three stages of matter. In state of solid, conduction arises by cause of vibration of particles and the energy transferred by free electrons. While in state of liquid and gases, it is realized by collision and diffusion of the random particles.

2.17.2 Convection

The second mechanism of heat flow is termed as convection which deals with the energy transfer because of particles's movement. This technique includes both the fluid particles's motion and conduction.There is direct relationship between fluid particles's motion and convective heat transfer. Furthermore, convection is named as forced convection if th external source or medium is responsible for the fluid flow. External medium involves wind(air), pump, fan or may be due to stretching surface. Against to forced convection, free convection (or natural convection) arises as result of buoyancy forces. These forces are generated by density variations in fluid flow because of temperature and absence of external sources $i.e$, stretching and magnetic force. Type of convection which involves the combine effects of forced and natural convection is called mixed convection.

2.17.3 Radiation

The mechanism in which energy transport takes place from any substance through emission (or absorption) of electromagnetic waves is termed as radiation. Particularly, radiation is significant throughout the process of combustion where temperature rises and it also occurs at room temperature. Radiative heat process does not depend upon any medium to propagate as in case of convection and conduction.

2.18 Stratification

Sometimes the mechanism of deformable density happened/appeared in the shallow fluid medium owing to change in the state of concentration, pressure, temperature and dissolved substances termed as stratification. It is witnessed that in case of stratification, density is the function of space variable as well as time. By cause of which layer formation occurs. Following are the two subclasses of stratification.

2.18.1 Thermal stratification

It happens as result of temperature imbalance, which provide rise to density imbalance in the fluid medium. Commomly, the reasons are thermal energy from heated bodies *e.g,* sun. When sunlight falls on lake's surface it assess change in temperature. The change in temperature depends on the lake's depth and degree that is able to influence by wind and any source of heated bodies. When lake is stratified, three layers arise inside the lake, the upper warm layer associated to as epilimnion, and the deeper cold layer referred to as hypolimnion. The boundary layer between the two layers where temperature changes more rapidly reffered to as thermocline. It is also noticed that temperature imbalance may changes from layer to layer and these flows have wider applications in agriculture and oceanography.

2.18.2 Concentration stratification

This type of stratification has application in many mechanism like transportation in the sea where stratification occurs due to salinity imbalance. As a result of existence of various fluids, a stable standpoint arises when the lighter fluids stands over the denser one.

2.19 Dimensionless numbers

2.19.1 Reynolds number

A dimensionless number used to identify flow pattern for different fluid flow occurrences like turbulant and laminar flow. It computes the ratio of inertial to viscous forces and relative significance of the two forces for given flow conditions. It is represented by Re termed after Osborne Reynolds,and is given as:

$$\mathrm{Re} = \frac{\text{inertial force}}{\text{viscous force}}. \tag{2.26}$$

$$\mathrm{Re} = \frac{\rho v^2/L}{\mu v/L^2} = \frac{vL}{\nu}. \tag{2.27}$$

Here, v represents the velocity of fluid, L denotes the characteristic length and ν describes kinematic viscosity. For low Reynolds number, flow is generally categorized as laminar flow. In laminar flow, fluid is moving with constant velocity and viscous forces are more dominant than inertial forces. Similarly, in case of higher Reynolds number, inertial forces are more significant than viscous forces, hence turbulant flow arises.

2.19.2 Hartmann number

A dimensionless parameter used to determine relative importance of drag force resulting from magnetic and viscous forces.Also, Hartmann number describes the connection between viscosity and frictional force generated by magnetism. It plays essential role in the magneto-hydrodynamics. Hartman number is the ratio of magnetic to the viscous force *i.e.*

$$M = \frac{\sigma B_0^2}{\rho a}, \tag{2.28}$$

where B_0 describes the magnetic induction, L stands for characateristics length, σ stands for resistivity and μdenotes viscosity.

2.19.3 Skin friction coefficient

When fluid is passed across a surface then certain amount of drag forces become apparant.These drag forces are termed as Skin friction. It happens between the fluid and the solid's surface which leads to slow down the fluid motion. The Skin friction coefficient can be expressed as:

$$C_f = \frac{2\tau_w}{\rho U_w^2}, \tag{2.29}$$

where τ_w (shear stress at the wall), ρ (fluid density) and U_w (velocity at wall) are the parameters on which Skin friction depends. Rise in Skin friction describes that how much drag obtains from the viscous stresses at the boundary. Laminar flow have less drag as compared to turbulant flow. To minimize Skin friction, it is mandatory to turn turbulant flow to laminar flow.

2.19.4 Lewis number

It describes the thermal diffusivity to Brownian diffusivity ratio. Mathematically, it is given by:

$$Le = \frac{\text{Thermal diffusitivity}}{\text{Brownian diffusivity}} = \frac{\alpha}{D_B}, \tag{2.30}$$

where α depicts thermal diffusivity and D_B describes Brownian diffusivity. Molecular diffusivity decreases when Lewis number increases.

2.19.5 Thermophoresis parameter

Thermophoresis parameter is positive and negative for cold and hot surface repectively. For hot surface, thermophoresis moves the nanoparticle concentration boundary layer away from the wall. As a result, a particle-free layer is formed at the boundary and therefore the nanoparticle distribution is obtained just outside. Mathematically, it can be expressed as:

$$N_t = \frac{\tau D_T (T_w - T_\infty)}{\nu T_\infty}, \tag{2.31}$$

in which T_w and T_∞ represents the wall temperature and temperature outside the plate, D_T describes thermophoretic diffusion coefficient and ν shows kinematic viscosity.

2.19.6 Brownian motion parameter

Irregular movement of suspended nanoparticles in a base fluid is named as Brownian motion. Brownian motion of nanoparticles is due to their random motion in base fluid produces from collision of nanoparticles with the base fluid. Such motion is because of size of the nanoparticles varying the heat transfer properties.

Mathematically,

$$N_b = \frac{\tau D_B (C_w - C_\infty)}{\nu}, \tag{2.32}$$

where τ is the ratio of effective heat and heat capacity of the nanoparticles and fluid respectively, ν stands for Kinematic viscosity. C_w describes the walls concentration, C_∞ denotes ambient concentration and and D_B represents the Brownian diffusion coefficient.

2.19.7 Grashof number

It describes the buoyancy forces to viscous forces ratio. Mathematically,

$$Gr_x = \frac{g\beta_T (T_w - T_\infty) x^3}{\nu}, \tag{2.33}$$

where g denotes gravitational constant, β_T stands for the coefficient of thermal expansion, ν is the kinematic velocity. T_w and T_∞ are the lower and upper temperatures at the channel walls.

2.19.8 Williamsons parameter

It studies the viscoelastic flows. It provides the relation of stress relaxation time and specific process time. It is abbreviated as We, and is mathematocally defines as:

$$We = U_w \Gamma \sqrt{\frac{2c}{\nu}}. \tag{2.34}$$

2.19.9 Biot number

Biot number is a dimensionless quantity which finds connection between the resistance of internal substance to the resistance at the surface of the substance. Mathematically,

$$\text{Biot number} = \frac{\text{Resistance of internal substance}}{\text{Resistance of surface of substance}},$$

$$\gamma^* = \frac{h_t}{k}\sqrt{\frac{\nu}{a}}, \tag{2.35}$$

where k stands for thermal conductivity, h_t denotes heat transfer coefficient and ν is kinematic viscosity.

2.19.10 Prandtl number

Prandtl number is used to compute the ratio of momentum diffusivity (kinematic viscosity ν) to thermal diffusivity (α). It is also stated as the product of dynamic viscosity (μ) and the specific heat capacity (c_p) at constant pressure to the thermal conductivity (k). Mathematically,

$$\text{Pr} = \frac{\text{Momentum diffusion rate}}{\text{Thermal diffusion rate}},$$

$$\text{Pr} = \frac{\nu}{\alpha} = \frac{\mu c_p}{k}, \tag{2.36}$$

where μ stands for dynamic viscosity, c_p describes the specific heat and k represents thermal conductivity. For the case when $\text{Pr} < 1$,thermal diffusion rate dominates while momentum diffusion rate dominates for $\text{Pr} > 1$. i.e in heat transfer, Prandtl number is used to control the thicknesses of momentum and thermal boundary layers.

2.20 Fundamental Conservation laws

The basic equations which are used for describing flow in the upcoming chapters are given below

2.20.1 Continuity Equation

This equation is derived from law of conservation of mass. Mathmatically, it is expressed as

$$\rho_t + \nabla.(\rho \mathbf{V}) = 0, \tag{2.37}$$

where ρ denotes density,$\mathbf{V} = (u, v, w)$ is the velocity field and t stands for time. For an incompressible fluid above equation turns to:

$$\nabla.\mathbf{V} = \mathbf{0}. \tag{2.38}$$

This form of continuity specify the source's absence in control volume.

2.20.2 Momentum Equation

Law of conservation of momentum plays a vital role in fluid mechanics and can be obtained with the help of Newton's second law of motion for an arbitrary control volume. Differential expression of momentum equation in vector form is given by:

$$\rho\frac{d\mathbf{V}}{dt} = \boldsymbol{\nabla}.\tau + \rho b. \tag{2.39}$$

The cauchy stress Tensor is given by:

$$\tau = -pI + S, \tag{2.40}$$

where p represents pressure, I stands for identity tensor, S describes the extra stress tensor, b denotes body force and d/dt is material time derivative. For the three dimensional flow, the cauchy stress tensor and the velocity of the field can be expressed as:

$$\tau = \begin{bmatrix} \sigma_{xx} & \tau_{xy} & \tau_{xz} \\ \tau_{yx} & \sigma_{yy} & \tau_{yz} \\ \tau_{zx} & \tau_{zy} & \sigma_{zz} \end{bmatrix}. \tag{2.41}$$

$$\mathbf{V} = [u(x, y, z), v(x, y, z), w(x, y, z)], \tag{2.42}$$

where σ_{xx}, σ_{yy} and σ_{zz} describes the normal stresses, all $\tau's$ represent the stear stresses and u, v, w are the velocity components along x, y and $z-$direction respectively.

2.20.3 Energy Equation

Energy equation may be obtained by applying the first law of thermodynamics to a control volume. It describes that changes in energy, heat transferred and work done by a system are in balance. Law of conservation of energy is also known as energy equation and is defined as total energy is conserved at the whole system. For a fluid with constant thermal conductivity, the basic energy equation for steady flow in the form of vector is given by:

$$\rho\frac{d\mathbf{e}}{dt} = \boldsymbol{\tau}.\mathbf{L} - \boldsymbol{\nabla}.\mathbf{q}_1 + \rho r_h, \tag{2.43}$$

where $\mathbf{e} = c_p T$ describes specific internal energy, c_p is the specific heat, T is the temperature, $\mathbf{L} = \boldsymbol{\nabla}\mathbf{V}$ the velocity gradiant, $\mathbf{q}_1 = -k\boldsymbol{\nabla}T$ stands for heat flux, k is thermal conductivity and r_h denotes radiative heating. Energy equation in the absence of thermal radiation is given by:

$$\rho c_p\frac{dT}{dt} = \boldsymbol{\tau}.\boldsymbol{\nabla}\mathbf{V} + k\boldsymbol{\nabla}^2 T. \tag{2.44}$$

2.20.4 Diffusion Equation

Mass transfer takes place whenever fluid flows $i.e$, some mass is transferred from one place to another place. According to Fick's law

$$\frac{dC}{dt} = \mathbf{D}_e\boldsymbol{\nabla}^2\mathbf{C} + k_n C_n, \tag{2.45}$$

in which C represents concentration, D_e stands for the coefficient of mass diffusivity and k_n is the reaction rate of diffusivity species.

2.21 Solution Methodology

In fluid mechanics physical problem are always non-linear. Exact solutions for such problems are not easy to find. Hence, some researchers turn to a numerical and approximate solutions. Amongst the various techniques there is one called homotopy analysis method. There is the development of series solution in this technique.

2.22 Homotopy

Homotopy is an essential concept of topology. Two functions are known as homotopic if one function can be deformed continuously into the other function. Two continuous maps ($f_1$and f_2) from the topological space A into the topological space B are called homotopic if there exists a continuous map F

$$F : A \times [0,1] \rightarrow B, \tag{2.46}$$

such that for each $a \in A$

$$F(a,0) = f_1(a), \tag{2.47}$$

$$F(a,1) = f_2(a). \tag{2.48}$$

The map F is known as homotopy between f_1 and f_2.

2.23 Homotopic solutions

Homotopy Analysis Method (HAM) is used to obtain the series solutions of highly nonlinear problems. It gives us convergent series solutions for highly nonlinear systems. For the basic concept of homotopy analysis method, we take into account a differential equation

$$\mathcal{N}\left[f\left(x\right)\right] = 0, \tag{2.49}$$

in which $\mathcal{N}$ denotes non-linear operator, $f\left(x\right)$ stands for unknown function while x describes the independent variable. Zeroth-order problem is given as follows:

$$\left(1 - Þ\right)\mathcal{L}\left[\tilde{f}\left(x; Þ\right) - f_0\left(x\right)\right] = Þ\hbar\mathcal{N}\left[\tilde{f}\left(x; Þ\right)\right], \tag{2.50}$$

where $f_0\left(x\right)$ denotes initial approximation, $\mathcal{L}$ stands for the characteristic linear operator, Þ $\in [0,1]$ shows an embedding parameter, $\hbar$ stands for non-zero auxiliary parameter and $\tilde{f}\left(x; Þ\right)$ is the unknown function of x and Þ.

Letting Þ = 0 and Þ = 1, we have

$$\tilde{f}(x;0) = f_0(x) \quad \text{and} \quad \tilde{f}(x;1) = f(x). \tag{2.51}$$

The solution $\tilde{f}(x;Þ)$ transforms from initial approximation $f_0(x)$ to the desired final solution $f(x)$ when Þ goes from 0 to 1. Using Taylor series expansion, we have

$$\tilde{f}(x;Þ) = f_0(x) + \sum_{m=1}^{\infty} f_m(x) Þ^m, \quad f_m(x) = \frac{1}{m!} \frac{\partial^m \tilde{f}(x;Þ)}{\partial Þ^m}\bigg|_{Þ=0}. \tag{2.52}$$

For Þ = 1, we get

$$f(x) = f_0(x) + \sum_{m=1}^{\infty} f_m(x). \tag{2.53}$$

Differentiating m times the zeroth deformation $w.r.t$ to Þ then divided by $n!$ and finally putting Þ = 0, we have the mth order equation

$$\mathcal{L}\left[f_m(x) - \chi_m f_{m-1}(x)\right] = \hbar \mathcal{R}_m(x), \tag{2.54}$$

$$\mathcal{R}_m(x) = \frac{1}{(m-1)!} \frac{\partial^m \mathcal{N}\left[\tilde{f}(x;Þ)\right]}{\partial Þ^m}\bigg|_{Þ=0}, \tag{2.55}$$

where

$$\chi_m = \begin{cases} 0, & m \leq 1 \\ 1, & m > 1 \end{cases}. \tag{2.56}$$

Chapter 3

Impact of generalized Fourier's and Fick's laws on MHD 3D second grade nanofluid flow with variable thermal conductivity and convective heat and mass conditions

3.1 Mathematical formulation

In this chapter second grade nanoliquid flow over a bidirectional extended sheet with velocities and in the $x-$and $y-$directions is taken up for consideration, with corresponding velocities $u = ax$ and $v = by$, while a and b are constants.. Flow analysis is carried out in the existence of Brownian motion and thermophoresis impacts with variable thermal conductivity and convective heat and mass boundary conditions. Flow of fluid is electrically conducting as a result of constant applied magnetic field of strength B_0 in a direction normal to the surface along with $z-$axis.We consider smaller Reynolds number to neglect induced magnetic field. Morover, we also discussed thermal diffusion with heat flux's relaxation and concentration diffusions with relaxation of mass fluxes. The surrounding values C_∞ and T_∞ are taken from the contant

values of concentartion and temperature at stretched surfaceas $z \to \infty$. Keeping all above considerations in mind, the boundary layer equations of the considered model is expressed as:

$$u_x + v_y + w_z = 0, \tag{3.1}$$

$$uu_x + vu_y + wu_z = \nu u_{zz} + \frac{k_0}{\rho}\left[uu_{zzx} + wu_{zzz} - u_x u_{zz} - u_z w_{zz} - 2u_z u_{zx} - 2w_z u_{zz}\right] - \frac{\sigma B_0^2}{\rho}u, \tag{3.2}$$

$$uv_x + vv_y + wv_z = \nu v_{zz} + \frac{k_0}{\rho}\left[vv_{zzy} + wv_{zzz} - v_y v_{zz} - v_z w_{zz} - 2v_z v_{yz} - 2w_z v_{zz}\right] - \frac{\sigma B_0^2}{\rho}v, \tag{3.3}$$

$$\mathbf{q} + \lambda_E\left(q_t + V.\nabla\mathbf{q} - \mathbf{q}.\nabla V + (\nabla.V)\,\mathbf{q}\right) = -k\nabla T, \tag{3.4}$$

$$\mathbf{J} + \lambda_C\left(\mathbf{J}_t + V.\nabla\mathbf{J} - \mathbf{J}.\nabla V + (\nabla.V)\,\mathbf{J}\right) = -D_B\nabla C, \tag{3.5}$$

where $\mathbf{q}$ and $\mathbf{J}$ describes the normal heat and mass fluxes respectively. k, D_B, λ_E and λ_C are the fluid's thermal conductivity of the fluid, Brownian diffusion coefficient, heat flux's relaxation time and mass flux's relaxation respectively. When $\lambda_E = \lambda_C = 0$, Eqs.(3.4) and (3.5) describes the classical Fourier and Fick laws respectively. Letting $\nabla.V = 0$ and the steady laminar flow with $\mathbf{q}_t = \mathbf{J}_t = 0$, Eqs.(3.4) and (3.5) becomes

$$\mathbf{q} + \lambda_E\left(V.\nabla\mathbf{q} - \mathbf{q}.\nabla V\right) = -\nabla\left(\alpha T\right), \tag{3.6}$$

$$\mathbf{J} + \lambda_C\left(V.\nabla\mathbf{J} - \mathbf{J}.\nabla V\right) = -D_B\nabla C. \tag{3.7}$$

Holding all above considerations and the impacts of Brownian motion and thermophoresis in mind, Eqs.(3.6) and (3.7) take the form

$$uT_x + vT_y + wT_z + \lambda_E\phi_E = \frac{1}{\rho c_p}\frac{\partial}{\partial z}\left(\alpha T_z\right) + \tau\left[D_B C_z T_z + \frac{D_T}{T_\infty}\left(T_z\right)^2\right], \tag{3.8}$$

$$uC_x + vC_y + wC_z + \lambda_C\phi_c = D_B C_{zz} + \frac{D_T}{T_\infty}T_{zz}, \tag{3.9}$$

where

$$\phi_E = u^2 T_{xx} + v^2 T_{yy} + w^2 T_{zz} + 2uvT_{xy} + 2uwT_{xz} + 2vwT_{yz}$$

$$+ \left(uu_x + vu_y + wu_z\right) T_x + \left(uv_x + vv_y + wv_z\right) T_y + \left(uw_x + vw_y + ww_z\right) T_z, \tag{3.10}$$

and

$$\phi_c = u^2 C_{xx} + v^2 C_{yy} + w^2 C_{zz} + 2uvC_{xy} + 2uwC_{xz} + 2vwC_{yz}$$

$$+ \left(uu_x + vu_y + wu_z\right) C_x + \left(uv_x + vv_y + wv_z\right) C_y + \left(uw_x + vw_y + ww_z\right) C_z, \tag{3.11}$$

with $\nu,\ T,\ c_p,\ \rho,\ D_B$ and D_T describes the kinematic viscosity, temperature, specific heat, fluid density, Brownian diffusion and thermo diffusion coefficients respectively. The subjected boundary conditions are:

$$u = U_w,\ v = V_w,\ w = 0,\ -kT_z = h_t\left(T_w - T\right),\ -D_B C_z = h_c\left(C_w - C\right),\ \text{at}\ \ z = 0,$$

$$u \to 0,\ v \to 0,\ T \to T_\infty,\ C \to C_\infty \text{ as } z \to \infty. \tag{3.12}$$

where h_t and h_c stands for the heat and mass transfer coefficients. For the solution of Eqs. (3.1) to (3.3) and Eqs. (3.8) and (3.9) with boundary conditions (3.12), we employ the following similarity transformations:

$$u = axf'\left(\eta\right),\ v = ayg'\left(\eta\right),\ w = -\sqrt{a\nu}\left(f\left(\eta\right) + g\left(\eta\right)\right), \tag{3.13}$$

$$\theta\left(\eta\right) = \frac{T - T_\infty}{T_w - T_\infty},\ \phi\left(\eta\right) = \frac{C - C_\infty}{C_w - C_\infty},\ \eta = \sqrt{\frac{a}{\nu}} z, \tag{3.14}$$

here " $\prime$ " shows the derivative $w.r.t$ "η". Considering thermal conductivity $k = k_a(1 + \alpha\theta\left(\eta\right))$ with $\alpha = (k - k_a)/k_a$ as reffered in [1] Eq. (3.1) is identically satisfied while Eqs. (3.2) to (3.5) are transformed to :

$$f''' - f'^2 + (f+g)f'' + \lambda^*\left[2\left(f' + g'\right)f''' - (f+g)f'''' - \left(f'' - g''\right)f''\right] - Mf' = 0, \tag{3.15}$$

$$g''' - g'^2 + (f+g)g'' + \lambda^* \left[2\left(f'+g'\right)g''' - (f+g)g'''' + \left(f''-g''\right)g''\right] - Mg' = 0, \tag{3.16}$$

$$(1+\epsilon\theta)\,\theta'' + \epsilon\theta'^2 + \Pr Nb\,\theta'\,\phi' + \Pr Nt\,\theta'^2 + \Pr(f+g)\,\theta'$$

$$-\delta_t \Pr\left((f+g)^2\,\theta'' + (f+g)\left(f'+g'\right)\theta'\right) = 0, \tag{3.17}$$

$$\phi'' + \frac{Nt}{Nb}\,\theta'' + \Pr Le\,(f+g)\,\phi' - \Pr Le\delta_c\left((f+g)^2\,\phi'' + (f+g)\left(f'+g'\right)\phi'\right) = 0, \tag{3.18}$$

and the boundary conditions take the form

$$f(0) = 0, \quad f'(0) = 1,\ g'(0) = \beta,\ g(0) = 0,$$

$$\theta'(0) = -\gamma_1^*\left(1-\theta(0)\right),\ \phi'(0) = -\gamma_2^*\left(1-\phi(0)\right),\ \text{at } z = 0,$$

$$f'(\infty) \to 0,\ g'(\infty) \to 0,\ \theta(\infty) \to 0,\ \phi(\infty) \to 0 \text{ as } z \to \infty. \tag{3.19}$$

Here, $M,\ \epsilon, \lambda^*,\ \Pr,\ Nb,\ Nt,\ Le,\ \delta_c,\ \delta_t,\ \beta,$ and $\gamma_1^*,\ \gamma_2^*,$ describe the Hartmann number, thermal conductivity parameter, second grade dimensionless parameter, Prandtl number, Brownian motion parameter, thermophoresis parameter, Lewis number, concentration relaxation parameter, thermal relaxation parameter, stretching ratio parameter and heat and mass transfer Biot numbers respectively. These parameters are given by:

$$Pr = \frac{\mu c_p}{k},\ Nt = \frac{\tau D_T(T_w - T_\infty)}{T_\infty \nu},\ Nb = \frac{\tau D_B\,(C_w - C_\infty)}{\nu},\ M = \frac{\sigma B_0^2}{\rho a},$$

$$Le = \frac{\alpha}{D_B},\ \delta_c = \lambda_C a,\ \gamma_1^* = \frac{h_t}{k}\sqrt{\frac{\nu}{a}},\ \beta = \frac{b}{a},\ \gamma_2^* = \frac{h_c}{D_B}\sqrt{\frac{\nu}{a}},\ \delta_t = \lambda_E a. \tag{3.20}$$

Description of Skin friction coefficients C_{f_x} and C_{f_y} in the x- and $y-$directions are given by:

$$C_{f_x} = \frac{\tau_{wx}}{\rho U_w^2},\ C_{f_y} = \frac{\tau_{wy}}{\rho U_w^2}, \tag{3.21}$$

with τ_{wx} and τ_{wy} are expressed as:

$$\tau_{wx}|_{z=0} = \mu u_z + k_0\left[u u_{xz} + v u_{yz} + w u_{zz} + u_z u_x + v_z v_x - w_z u_z\right]_{z=0}, \tag{3.22}$$

$$\tau_{wy}\big|_{z=0} = \mu v_z + k_0 \left[u v_{xz} + v v_{yz} + w v_{zz} + u_z u_y + v_z v_y - w_z v_z \right]_{z=0}. \tag{3.23}$$

Dimensionless forms of Skin friction coefficients are defined by:

$$C_{f_x} Re^{1/2} = \left[f'' + K \left(2 f' f'' - (f+g) f''' + \left(f' + g' \right) f'' \right) \right]_{\eta=0} \ , \tag{3.24}$$

$$C_{f_y} Re^{1/2} = \left[g'' + K \left(2 g' g'' - (f+g) g''' + \left(f' + g' \right) g'' \right) \right]_{\eta=0}, \tag{3.25}$$

where $\mathrm{Re}_x = \frac{u_w x}{\nu}$.

3.2 Homotopic solutions

Homotopy Analysis method (HAM) was suggested by Liao [35] in 1992 for the solution of highly nonlinear differential equations. This technique has an edge over rest of the contemporary techniques on account of ensuing characteristics:

i) It is free from selection of small or large parameters.

ii) Guaranteed the convergence of series solution.

iii) Provides sufficient choice for choosing initial guess estimates and operators.

For the problem under consideration, initial guess estimates $(f_0, g_0, \theta_0, \phi_0)$ are taken as:

$$f_0(\eta) = (1 - \exp(-\eta)), \ g_0(\eta) = \beta (1 - \exp(-\eta)),$$
$$\theta_0(\eta) = \frac{\overset{*}{\gamma}_1}{1 + \overset{*}{\gamma}_1} \exp(-\eta), \ \phi_0(\eta) = \frac{\overset{*}{\gamma}_2}{1 + \overset{*}{\gamma}_2} \exp(-\eta), \tag{3.26}$$

which are supported by the following linear operators:

$$\mathcal{L}_f(\eta) = \frac{d^3 f}{d\eta^3} - \frac{df}{d\eta}, \ \mathcal{L}_g(\eta) = \frac{d^3 g}{d\eta^3} - \frac{dg}{d\eta}, \tag{3.27}$$

$$\mathcal{L}_\theta(\eta) = \frac{d^2 \theta}{d\eta^2} - \theta, \ \mathcal{L}_\phi(\eta) = \frac{d^2 \phi}{d\eta^2} - \phi, \tag{3.28}$$

with the following characteristics

$$\mathcal{L}_f \left[C_1 + C_2 \exp(\eta) + C_3 \exp(-\eta)\right] = 0, \tag{3.29}$$

$$\mathcal{L}_g \left[C_4 + C_5 \exp(\eta) + C_6 \exp(-\eta)\right] = 0, \tag{3.30}$$

$$\mathcal{L}_\theta \left[C_7 \exp(\eta) + C_8 \exp(-\eta)\right] = 0, \tag{3.31}$$

$$\mathcal{L}_\phi \left[C_9 \exp(\eta) + C_{10} \exp(-\eta)\right] = 0, \tag{3.32}$$

in which C_i $(i = 1 - 10)$ are the arbitrary constants. The values of these constants through the boundary conditions are

$$\begin{aligned} C_2 = C_5 = C_7 = C_9 = 0,\ C_3 = \left.\frac{\partial f_m^\star(\eta)}{\partial \eta}\right|_{\eta=0},\ C_1 = -C_3 - f_m^\star(0), \\ C_4 = -C_6 - g_m^\star(0),\ C_6 = \left.\frac{\partial g_m^\star(\eta)}{\partial \eta}\right|_{\eta=0}, \\ C_8 = -\theta_m^*(0),\ C_{10} = -\phi_m^*(0). \end{aligned} \tag{3.33}$$

3.3 Convergence analysis

It is important to find convergence regions of all the involved distributions for convergent series solutions. These convergent regions depend upon the calculations of the auxiliary parameter $\hbar$. Figure 3.1 represents the $\hbar-$curves behavior for all distributions. The desirable ranges of these parameters $\hbar_f$, $\hbar_\theta$ and $\hbar_\phi$ are $-1.5 \leq \hbar_f \leq -0.4$, $-1.4 \leq \hbar_g \leq -0.4$, $-1.4 \leq \hbar_\theta \leq -0.4$ and $-1.6 \leq \hbar_\phi \leq -0.5$. Table 3.1 displays the convergence of the considered method mathematically. It can be verified that both presented Fig. 3.1 and Table 3.1 values are in total alignment.

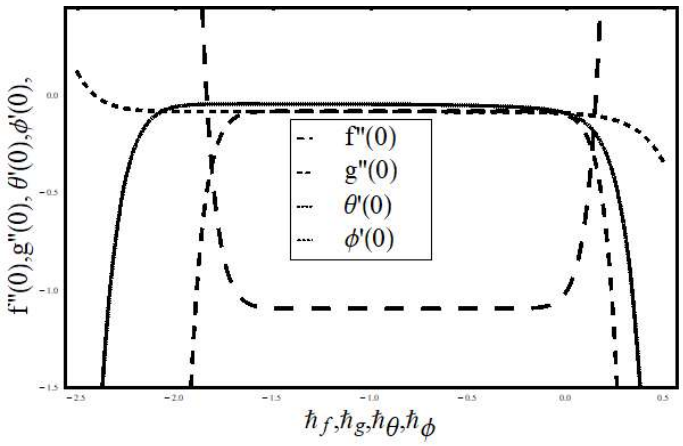

Fig. 3.1 $\hbar-$curves for f, g, θ, ϕ

Table 3.1. Convergence of series solutions for different order of approximations when $\lambda^* = 0.1,\ M = 0.3, \overset{*}{\gamma_1} = \overset{*}{\gamma_2} = 0.1, Nt = 0.8,\ N_b = 0.2,\ Le = 1.0,\ \delta_t = \delta_c = 0.2,\ \Pr = 1.0, \epsilon = \beta = 0.1$

Order of approximations	$-f''(0)$	$-g''(0)$	$-\theta'(0)$	$-\phi'(0)$
1	1.06300	0.07450	0.08761	0.07130
5	1.09234	0.07821	0.08382	0.05675
10	1.09342	0.07809	0.08235	0.04913
15	1.09343	0.07809	0.08187	0.04549
20	1.09343	0.07809	0.08169	0.04370
25	1.09343	0.07809	0.08161	0.04281
30	1.09343	0.07809	0.08159	0.04256
35	1.09343	0.07809	0.08159	0.04256

3.4 Results and Discussion

This section is concerned to study the influence of appearing parameters on respective distributions through figures $3.2 - 3.19$. Figures 3.2 and 3.3 describes $\beta's$ (stretching rate ratio) behavior on velocity profiles. It is observed that both velocities show conflicting behavior in $x-$ and $y-$directions for an increasing rate of β. As $\beta = b/a$, a is smaller for higher values

of β that specifies decreasing rate in velocity along $x-$axis or higher values of b that indicates increasing rate along $y-$axis. Figure 3.4 has drawn to depict the impact of second grade parameter λ^* on velocity field. It is indicated that moderate increment in λ^* give support to velocity profile. This is the result of the fact that enhanced flow of fluid has dependency on higher values of λ^*. It is also noticed that the current problem may be deformed into viscous fluid case by setting $\lambda^* = 0$. In figure 3.5 the effect of Prandtl number Pr on temperature profile is presented. It is to be noted that for higher values of Pr, diffusion of heat from the heated surface is very slow in comparison to smaller values of Pr. Therefore, decrease in temperature is preceived against associated values of Pr. Figures 3.6 and 3.7 are drawn to understand the influences of thermal and concentration relaxations parameters δ_t and δ_c on concentration and temperature distributions are shown respectively. It is observed that both concentration temperature fields with associated boundary layer thicknesses are decreasing functions of δ_t and δ_c respectively. Furthermore, for $\delta_t = 0$ and $\delta_c = 0$, current model will transform to classical laws of Fourier's and Fick's respectively. Figure 3.8 describes the effect of thermal conductivity parameter ϵ on temperature profile. Higher values of ϵ causes increment for the thermal boundary layer. Due to which an increase in temperature distribution is detected. Figure 3.9 exhibits the influence of Lewis number Le on concentration field. Lesser values of mass diffusivity than thermal diffusivity results in stronger Lewis number. As a result, a weaker Brownian motion coefficient is witnessed that lowers the nanoparticle concentration profile. Figures 3.10 and 3.11 are drawn to illustrate the effect of Hartmann number M on both velocities profiles alomg $x-$ and $y-$directions. Retardation in the fluid's motion is observed because of resistance offered by strong Lorentz force. This act finally points out as decreament in both velocity distributions. Figures 3.12 and 3.13 are drawn to represent the influence of heat and mass Biot numbers $\overset{*}{\gamma}_1$ and $\overset{*}{\gamma}_2$ on temperature and concentration profiles respectively. It indicates that both temperature distribution and concentration distributions are increasing functions of $\overset{*}{\gamma}_1$ and $\overset{*}{\gamma}_2$. High dependency of $\overset{*}{\gamma}_1$ and $\overset{*}{\gamma}_2$ on respective heat and mass coefficients augment the associated temperature and concentration distributions for ascending values of respective Biot numbers. Figure 3.14 is drawn to reflect the effect of thermophoresis parameter Nt on temperature field. As we increase the value of Nt, movement of nanoparticles from hot to the cold ambient fluid is observed and results in higher values of temperature in the region

of the boundary layer. Eventually, augmented thermal boundary layer thickness is preceived. Figure 3.15 describes the effect of the thermophoresis parameter Nt on concentration field. Higher values of thermophoresis parameter Nt are in direct proportionate with temperature gradient which in turn boosts the concentration profile and its allied concentration boundary layer thickness. Figures 3.16 and 3.17 illustrates the impact of Brownian motion parameter Nb on temperature and concentration profiles. Higher values of Nb increase the temperature of the fluid in the boundary layer and instantaneously reduce particles's deposition far off from the fluid on the stretched surface. That's why temperature accelerates and concentration decelerates. Figure 3.18 is drawn for understanding the effects of second grade dimensionless parameter λ^* and stretching ratio parameter β on Skin friction coefficient along $y-$direction. It is preceived that Skin friction coefficient shows increasing behavior against both λ^* and β. Similar trend is seen in case of second grade dimensionless parameter λ^* and Hartmann number M versus Skin friction coefficient along $x-$ direction. This impact is presented in figure 3.19.

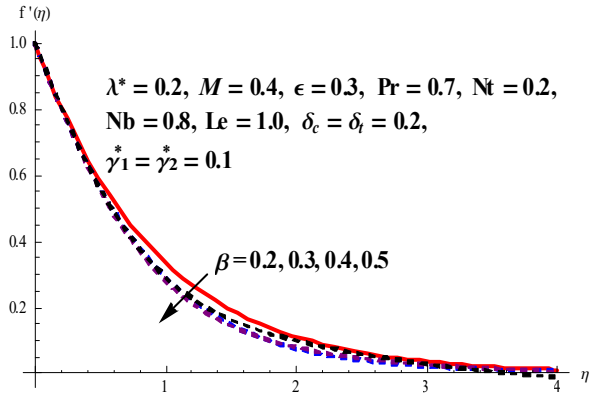

Fig 3.2. Impact of β on f'

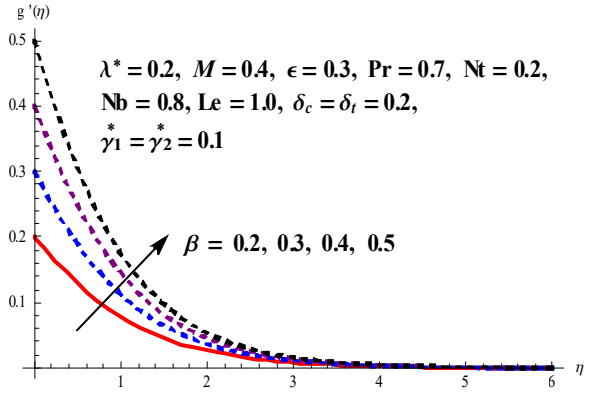

Fig 3.3 Impact of β on g'

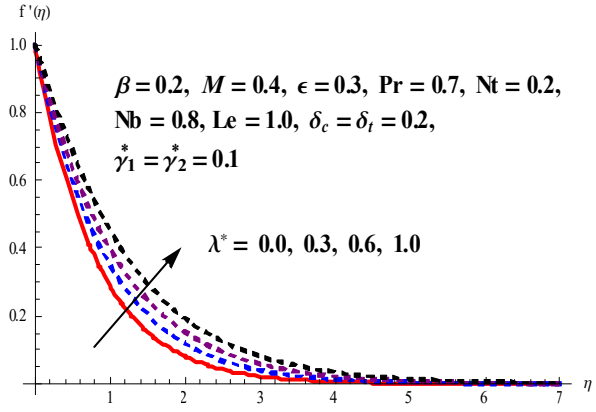

Fig 3.4. Impact of λ^* on f'

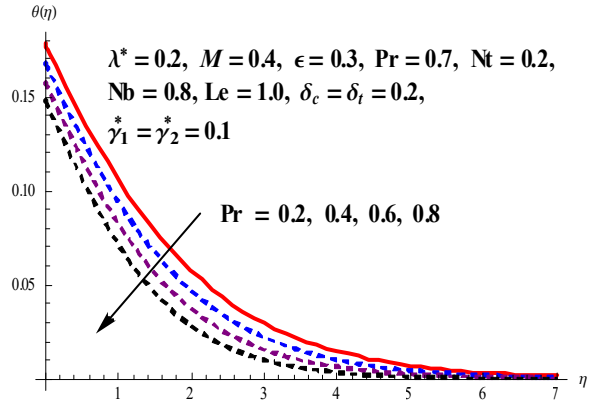

Fig 3.5. Impact of Pr on θ

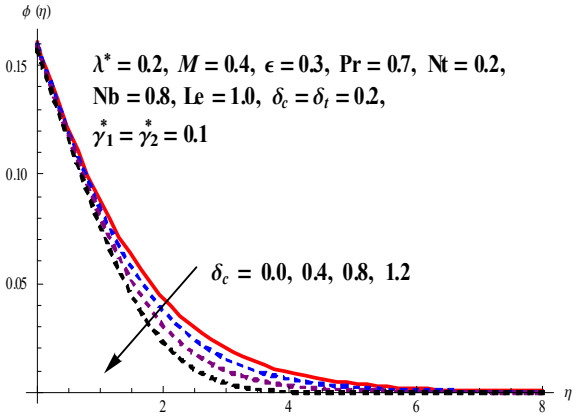

Fig 3.6. Impact of δ_c on ϕ

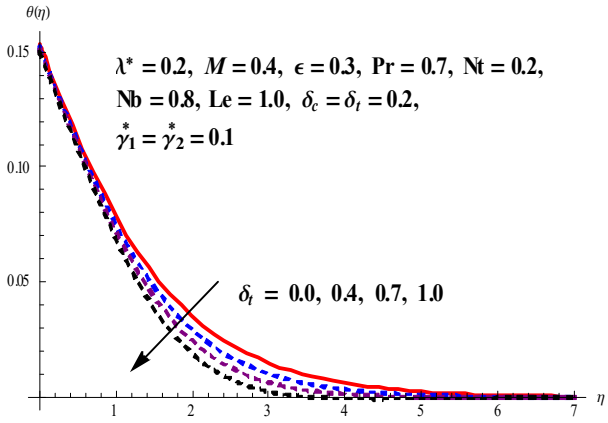

Fig 3.7. Impact of δ_t on θ

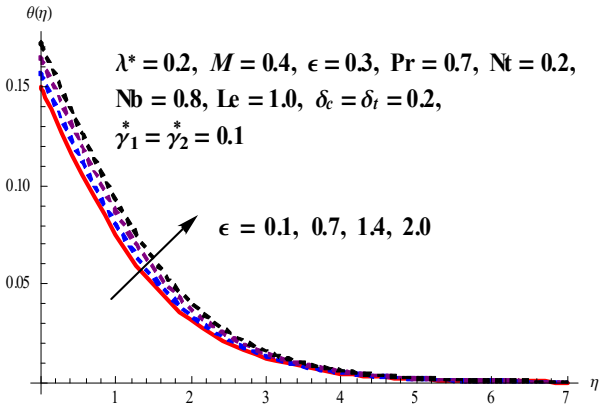

Fig 3.8. Impact of ϵ on θ

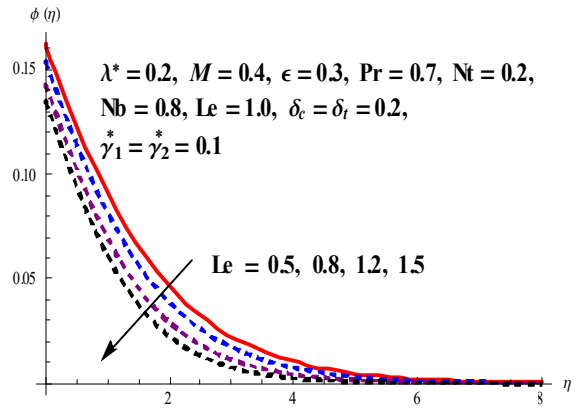

Fig 3.9. Impact of Le on ϕ

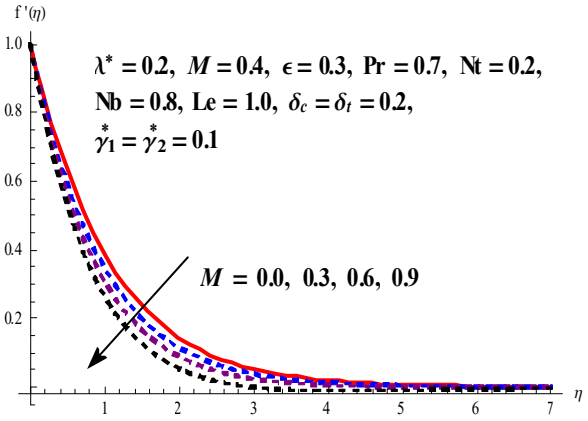

Fig 3.10. Impact of M on f'

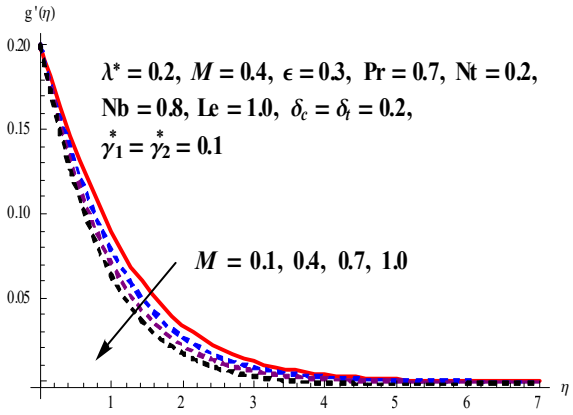

Fig 3.11. Impact of M on g'

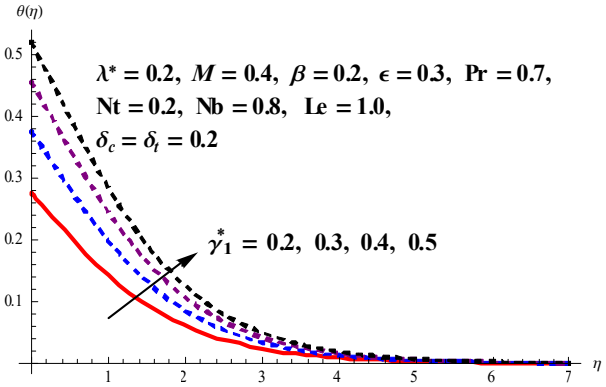

Fig 3.12. Impact ofγ_1^* on ϕ

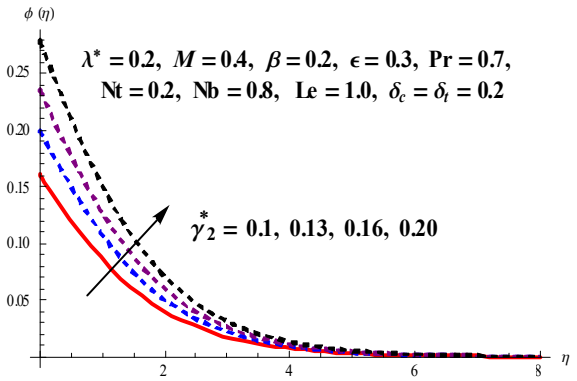

Fig 3.13. Impact of γ_2^* on ϕ

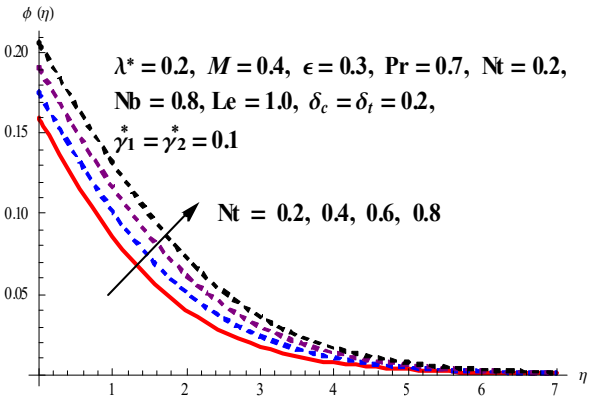

Fig 3.14. Impact of Nt on ϕ

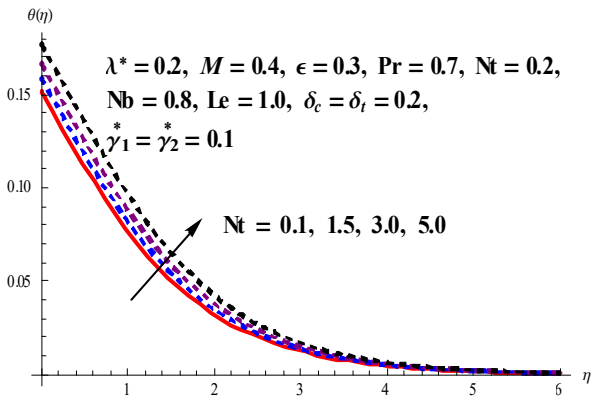

Fig 3.15. Impact of Nt on θ

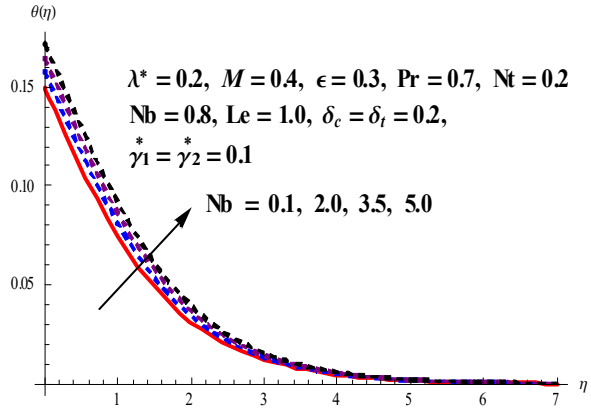

Fig 3.16. Impact of Nb on θ

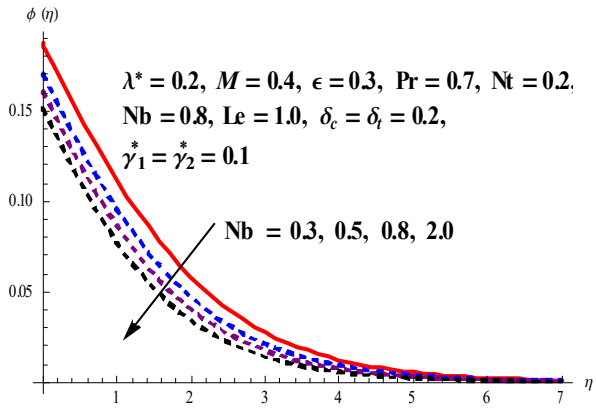

Fig 3.17. Impact of Nb on ϕ

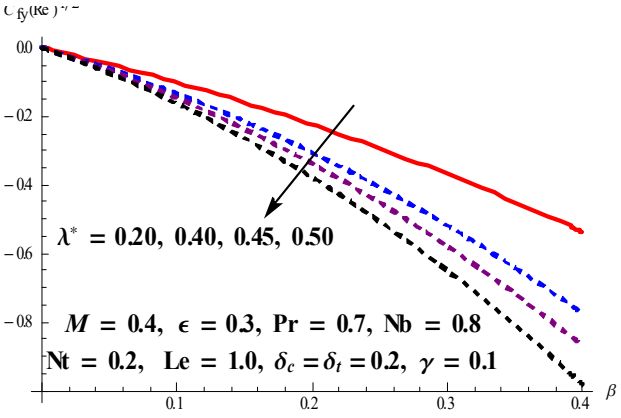

Fig 3.18. Impact of β and λ^* on $C_{f_y}(\mathrm{Re})^{1/2}$

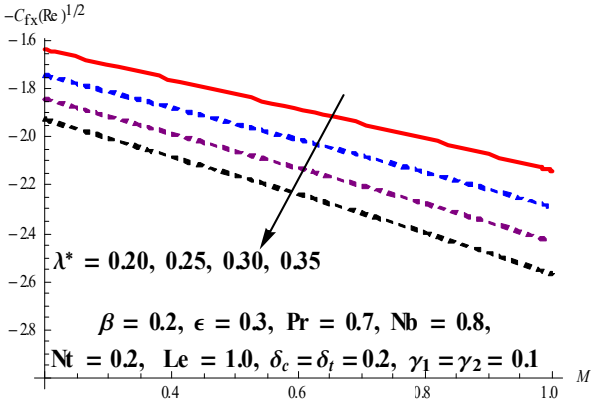

Fig 3.19.Impact of λ^* and M on $C_{f_x}(\mathrm{Re})^{1/2}$

To validate results of the present exploration, Table 3.2 displays comparision with frame work of Ahmad and Nazar [36] for skin friction in absence of nanofluid, variable thermal conductivity, cattaneo-Christov thermal and concentration diffusion fluxes and convective heat and mass boundary conditions. An excellent correlation is exhibited between both results.

Table 3.2: Comparison of varied values of $\boldsymbol{\beta}$ with Ahmed and Nazar [36].

		$\beta = 0$		$\beta = 0.5$				$\beta = 1$	
M	λ	[36]	Present	[36]		Present		[36]	Present
		$-f''$	$-f''$	$-f''$	$-g''$	$-f''$	$-g''$	$-g''$	$-g''$
0	0	1.0042	1.0046	1.0932	0.4653	1.0935	0.4656	1.1748	1.1750
	0.2	0.9225	0.9228	0.9291	0.4066	0.9294	0.4068	0.9444	0.9445
	1.0	0.7504	0.7506	0.6513	0.2943	0.6514	0.2945	0.6461	0.6464
10	0	3.3165	3.3170	3.3420	1.6459	3.3423	1.6461	3.3667	3.3669
	0.2	3.0276	3.0278	2.8048	1.3840	2.8050	1.3843	2.6317	2.6320
	1.0	2.3452	2.3455	1.9175	0.9482	1.9176	0.9484	1.6667	1.6669
100	0	10.0498	10.050	10.0582	5.0208	10.0585	5.0210	10.0663	10.0666
	0.2	9.1742	9.1745	8.4315	4.2096	8.4318	4.2097	7.8471	7.8472
	1.0	7.1063	7.1066	5.7552	2.8741	5.7554	2.8744	4.9551	4.9553

Chapter 4

Upshot of generalized Fourier's and Fick's laws on MHD Williamson nanofluid flow past a bi-directional stretched surface with second order slip and double stratification

4.1 Mathematical formulation

Here, the steady 3D williamson nanoliquid flow over a bidirectional extended sheet with velocities $u = ax$ and $v = by$ and in the $x-$ and $y-$directions is taken up for consideration. Thermal and concentration buoyancy forces are applied to the fluid with double stratified phenomena to study heat and mass transfers.

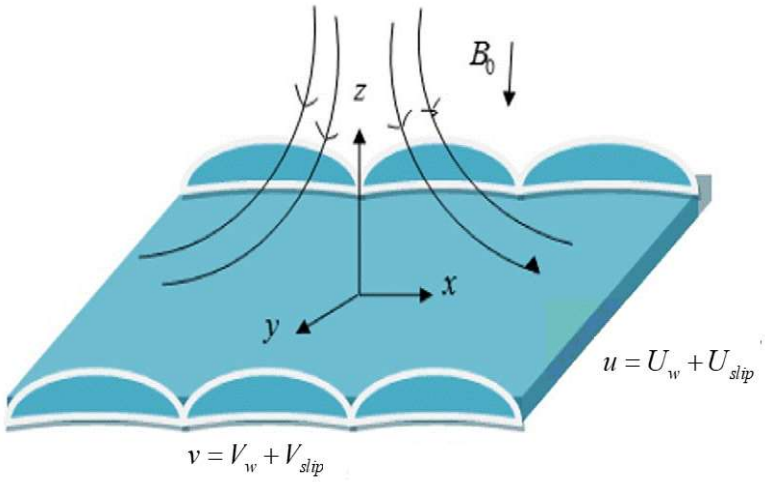

Figure 4.1. Schematic Diagram

By applying boundary layer approximations, the governing equations are expressed as follows:

$$u_x + v_y + w_z = 0, \tag{4.1}$$

$$uu_x + vu_y + wu_z = \nu u_{zz} + \sqrt{2}\nu\Gamma u_z u_{zz} - \frac{\sigma B_0^2}{\rho}u + \begin{bmatrix} g\ [\alpha_1(T - T_\infty) + \alpha_2(T - T_\infty)^2] + \\ g\ [a_3(C - C_\infty) + \alpha_4(C - C_\infty)^2] \end{bmatrix}, \tag{4.2}$$

$$uv_x + vv_y + wv_z = \ \nu v_{zz} + \sqrt{2}\nu\Gamma v_z v_{zz} - \frac{\sigma B_0^2}{\rho}v, \tag{4.3}$$

$$q + \lambda_E(\mathbf{q}_t + V.\boldsymbol{\nabla}\mathbf{q} - \mathbf{q}.\nabla V + (\nabla.V)\mathbf{q}) = -\nabla(kT), \tag{4.4}$$

$$J + \lambda_C(J_t + V.\nabla J - J.\nabla V + (\nabla.V)J) = -D_B\nabla C, \tag{4.5}$$

where $\lambda_C, \lambda_E, J, \sigma, \rho$ and ν are the mass flux's relaxation time, heat flux's relaxation time , mass flux,electrical conductivity, density of fluid and kinematic viscosity respectively. For $\lambda_E = \lambda_C = 0$, above equations represent the classical laws of Fick and Fourier, respectively. Assuming $\nabla.V = 0$ and the time independent laminar flow with $\mathbf{q}_t = J_t = 0$,then the above equation becomes

$$q + \lambda_E(V.\nabla q - q.\nabla V) = -\nabla(kT), \tag{4.6}$$

$$J + \lambda_C(V.\nabla J - J.\nabla V) = -D_B \nabla C, \tag{4.7}$$

keep it in mind the above cosiderations and the impact of Brownian motion and the thermophoresis, Eqs (4.6) and (4.7) are given by

$$uT_x + vT_y + wT_z + \lambda_E \Phi_E = \frac{1}{\rho c_p}\frac{\partial}{\partial z}(kT_z) + \tau[D_B C_z T_z + \frac{D_T}{T_\infty}(T_z)^2, \tag{4.8}$$

$$uC_x + vC_y + wC_z + \lambda_C \Phi_C = D_B C_{zz} + \frac{D_T}{T_\infty} T_{zz}, \tag{4.9}$$

with

$$\Phi_E = u^2 T_{xx} + v^2 T_{yy} + w^2 T_{zz} + 2uvT_{xy} + 2uwT_{xz} + 2vwT_{yz} + (uu_x + vu_y + wu_z)T_x +$$

$$(uv_x + vv_y + wv_z)T_y + (uw_x + vw_y + ww_z)T_z, \tag{4.10}$$

and

$$\Phi_C = u^2 C_{xx} + v^2 C_{yy} + w^2 C_{zz} + 2uvC_{xy} + 2uwC_{xz} + 2vwC_{yz} + (uu_x + vu_y + wu_z)C_x +$$

$$(uv_x + vv_y + wv_z)C_y + (uw_x + vw_y + ww_z)C_z, \tag{4.11}$$

subjected to the boundary conditions

$$u = U_w + U_{slip}, \quad v = V_w + V_{slip}, \quad w = 0, \tag{4.12}$$

$$T = T_w = T_0 + d_1 x \ , \quad C = C_w = C_0 + d_2 x \qquad \text{at} \qquad z = 0, \tag{4.13}$$

$$u \to 0, \quad v \to 0, \ T \to T_\infty = T_0 + e_1 x, \ C \to C_\infty = C_0 + e_2 x \quad \text{at } z \to \infty, \tag{4.14}$$

where

$$\begin{aligned} Uslip &= \frac{2}{3}\left(\frac{3-\alpha l^3}{\alpha} - \frac{3}{2}\frac{1-l^2}{K_n}\right)\Lambda u_z - \frac{1}{4}\left(l^4 + \frac{2}{K_n^2}(1-l^2)\right)\Lambda^2 u_{zz}, \\ &= A u_z + B u_{zz}, \end{aligned} \tag{4.15}$$

$$\begin{aligned} Vslip &= \frac{2}{3}\left(\frac{3-\alpha l^3}{\alpha} - \frac{3}{2}\frac{1-l^2}{K_n}\right)\Lambda v_z - \frac{1}{4}\left(l^4 + \frac{2}{K_n^2}(1-l^2)\right)\Lambda^2 v_{zz}, \\ &= C v_z + D v_{zz}, \end{aligned} \tag{4.16}$$

with $l = \min[\frac{1}{k_n}, 1]$, α is momentum accommodation coefficient with $1 \geqslant \alpha \geqslant 0$, Λ is molecular mean free path and K_n knudsen number defined as mean free path Λ divided by a characteristic length for the flow. Based on the definition of l, it is seen that for any given values of K_n we have $1 \geqslant l \geqslant 0$. The molecular mean free path is always positive. Thus we know that B , D < 0, and C and A are positive numbers.

To solve above equations we introduce similarity transformations:

$$\begin{gathered} u = axf\,'(\eta), \qquad v = ayg'(\eta), \qquad w = -\sqrt{a\nu}(f(\eta) + g(\eta)), \\ \theta(\eta) = \frac{T - T_\infty}{T_w - T_\infty}, \qquad \phi(\eta) = \frac{C - C_\infty}{C_w - C_\infty}, \qquad \eta = \sqrt{\frac{a}{\nu}} z \ , \end{gathered} \tag{4.17}$$

Incompressibility condition is satisfied automatically and Equations (4.2) to (4.5) reduce to

$$f\,''' - f\,'^2 + (f+g)f\,'' + We\,f\,''f''' + \lambda(1+\beta_2\theta)\theta + \lambda Nr(1+\beta_3\phi)\phi - Mf\,' = 0, \tag{4.18}$$

$$g''' - g'^2 + (f+g)g'' + Weg''g''' - Mg' = 0, \tag{4.19}$$

$$\begin{gathered}(1+\epsilon\theta)\,\theta'' + \epsilon\theta'^2 + \Pr Nb\theta'\phi' + \Pr Nt\theta'^2 - \Pr f'(S_1+\theta) + \Pr(f+g)\,\theta' - \\ \delta_t \Pr \left(\begin{array}{c} (f+g)^2\theta'' - 2f'\theta'(f+g) + \left(f'^2 - f''(f+g)\right)(S_1+\theta) + \\ (f+g)(f'+g')\theta' \end{array} \right) = 0, \\ \phi'' + \frac{Nt}{Nb}\theta'' - \Pr Lef'(S_2+\theta) + \Pr Le(f+g)\phi' -\end{gathered} \tag{4.20}$$

$$\Pr Le\delta_c \left(((f+g)^2\phi'' - 2f'(f+g)\phi' + (f'^2 - f''(f+g))(S_2+\phi) + (f+g)(f\,'+g')\phi')\right) = 0, \tag{4.21}$$

with boundary conditions

$$f(0) = 0, \quad f'(0) = 1 + \gamma_1 f\,''(0) + \gamma_2 f\,'''(0), \quad g\,(0) = 0,$$

$$g'(0) = \beta + \gamma_3 f\,''(0) + \gamma 4 f\,'''(0),\ \theta(0) = 1 - S_1,\ \phi(0) = 1 - S_2,$$

$$f'(\infty) \to 0, \quad g'(\infty) \to 0 \qquad \theta\,(\infty) = 0, \quad \phi\,(\infty) = 0, \quad \text{as } z \to \infty, \tag{4.22}$$

where γ_4 and $\gamma_2(<0)$ are the the second order slip velocity paramerter and γ_3 and γ_1 are the first order slip parameter. β is the stretching ratio parameter, M is the Hartmann number, Nb and Nt are the brownian motion and thernophoresis parameters, δ_t and δ_c are the thermal relaxation and concentration relaxation parameters, Le is the Lewis number, Pr is the prandtl number, We is the williamsons parameter , Nr is the ratio of the concentration to thermal buoyancy forces, λ is the mixed convection parameter , Gr_x is the Grashof number for temperature , β_2, β_3 are the the non-linear temperature's convection parameter and non-linear concentration's convection parameter. Re_x is the local Reynold number. S_1 is the thermal

stratification parameter and S_2 is the solutal stratification parameter.

$$\lambda = \frac{Gr_x}{\mathrm{Re}_x^2}\ , \quad Gr_x = \frac{g\alpha_1\,(T_w - T_\infty)x^3}{\nu^2}, \quad \mathrm{Re}_x = \frac{u_w x}{\nu}, \quad Nr = \frac{\alpha_3(C_w - C_0)}{\alpha_1(T_w - T_0)}, \quad S_2 = \frac{e_2}{d_2},$$

$$\gamma_1 = A\sqrt{\frac{a}{\nu}}, \quad \gamma_2 = B\frac{a}{\nu}, \quad \gamma_3 = C\sqrt{\frac{a}{\nu}}, \quad \gamma_4 = D\frac{a}{\nu}, \quad \beta_2 = \frac{\alpha_2}{\alpha_1}(T_w - T_0), \quad S_1 = \frac{e_1}{d_1},$$

$$\beta_3 = \frac{\alpha_4}{\alpha_3}(C_w - C_0), \quad We = U_w\Gamma\sqrt{\frac{2c}{\nu}}, \quad \mathrm{Pr} = \frac{\mu c_p}{k}, \quad M = \frac{\sigma B_0^2}{\rho a}, \quad Le = \frac{\alpha}{D_B},$$

$$Nt = \frac{\tau D_T d_1 x}{T_\infty \nu}, \quad Nb = \frac{\tau D_B d_2 x}{T_\infty \nu}, \ \delta_c = \lambda_c a, \ \delta_t = \lambda_E a, \quad \beta = \frac{b}{a}. \tag{4.23}$$

Skin friction coefficients C_{f_x} and C_{f_y} in $x-$ and $y-$ direction are are represented as follows:

$$C_{f_x} = \frac{\tau_{wx}}{\rho U_w^2}, \qquad C_{f_y} = \frac{\tau_{wy}}{\rho U_w^2}, \tag{4.24}$$

where

$$\tau_{wx}\ |_{z=0} = u_z + \frac{\Gamma}{\sqrt{2}}(u_z)^2, \tag{4.25}$$

and

$$\tau_{wy}\ |_{z=0} = v_z + \frac{\Gamma}{\sqrt{2}}(v_z)^2, \tag{4.26}$$

Skin friction coefficients in dimensionless forms are:

$$C_{f_x}\,\mathrm{Re}^{1/2} = [f\,'' + \frac{We}{2}(f\,'')^2]_{\eta=0} \tag{4.27}$$

$$C_{f_y}\,\mathrm{Re}^{1/2} = [g'' + \frac{We}{2}(g'')^2]_{\eta=0} \tag{4.28}$$

where $\mathrm{Re}_x = U_w x/\nu$.

4.2 Homotopic solutions

For the considered problem the linear operators and the initial guesses $(f_0, g_0, \theta_0, \phi_0)$ and $(\mathcal{L}_f, \mathcal{L}_g, \mathcal{L}_\theta, \mathcal{L}_\phi)$ are expressed in the form:

$$f_0(\eta) = \frac{A}{1+\gamma_1-\gamma_2}\left(1-\exp(-\eta)\right), \quad g_0(\eta) = \frac{\beta}{1+\gamma_3-\gamma_4}\left(1-\exp(-\eta)\right),$$

$$\theta_0(\eta) = (1-S1)\exp(-\eta), \qquad \phi_0(\eta) = (1-S2)\exp(-\eta), \tag{4.29}$$

$$\mathcal{L}_f(f) = \frac{d^3f}{d\eta^3} - \frac{df}{d\eta}, \quad \mathcal{L}_g(g) = \frac{d^3g}{d\eta^3} - \frac{dg}{d\eta}, \tag{4.30}$$

$$\mathcal{L}_\theta(\theta) = \frac{d^2\theta}{d\eta^2} - \theta, \quad \mathcal{L}_\phi(\phi) = \frac{d^2\phi}{d\eta^2} - \phi, \tag{4.31}$$

with

$$\mathcal{L}_f\left[C_1 + C_2\exp(\eta) + C_3\exp(-\eta)\right] = 0, \tag{4.32}$$

$$\mathcal{L}_g\left[C_4 + C_5\exp(\eta) + C_6\exp(-\eta)\right] = 0, \tag{4.33}$$

$$\mathcal{L}_\theta\left[C_7\exp(\eta) + C_8\exp(-\eta)\right] = 0, \tag{4.34}$$

$$\mathcal{L}_\phi\left[C_9\exp(\eta) + C_{10}\exp(-\eta)\right] = 0, \tag{4.35}$$

where C_i $(i = 1-10)$ are the arbitrary constants. Following are the values of this constants :

$$C_2 = C_5 = C_7 = C_9 = 0,\ C_1 = -C_3 - temp, \quad C_3 = \frac{temp' - \gamma 1 temp'' - \gamma 2 temp'''}{1+\gamma 1 - \gamma 2}, \tag{4.36}$$

$$C_4 = -C_6 - temp, C_6 = \frac{temp' - \gamma 3 temp'' - \gamma 4 temp'''}{1+\gamma 3 - \gamma 4},\ \ C_8 - temp',\ \ C_{10} = -temp'. \tag{4.37}$$

4.3 Convergence analysis

Homotopy analysis technique is applied to obtain the series solutions of highly nonlinear problems which was suggested by Liao [35]. It provides a great freedom to adjust and control the convergence region of the series solutions.. Figure 4.2. represents the $\hbar-$curves behavior of all distributions The permissible ranges of the characteristic parameters $\hbar_f$, $\hbar_g, \hbar_\theta$ and $\hbar_\phi$ are $-1.6 \leq \hbar_f \leq -0.4, -2.15 \leq \hbar_g \leq -0.2, -2.75 \leq \hbar_\theta \leq -0.8$ and $-2.6 \leq \hbar_\phi \leq -0.6$ when $\gamma = 0.2$, $Nt = 0.2$, $Nb = 0.3$, $Le = 1.0$, $Pr = 1.0, \epsilon = 0.3$, $\lambda = 0.002$, $\beta_1 = \beta_3 = 0.2$, $\beta = 0.1$ and $M = 0.2$, Table 4.1 represents the convergence of considered method mathematically. It can be verified that both presented Fig. 4.2 and Table 4.1 values are in total allignment.

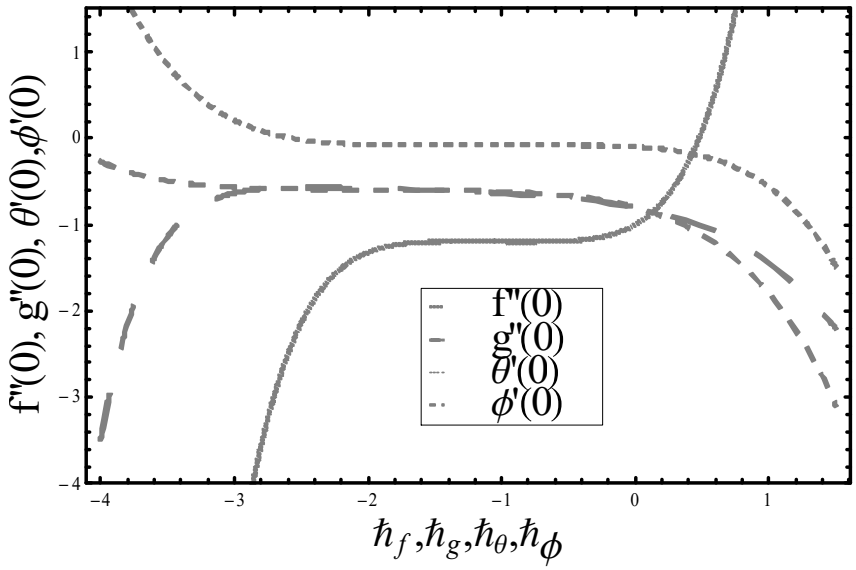

Fig.4.2. $\hbar-$curves for f, g, θ, ϕ

Table 4.1. Convergence of series solutions for different order of approximations when $\lambda = 0.002$, $M = 0.2$, $\gamma_1 = \gamma_2 = 0.2$, $Nt = 0.2$, $N_b = 0.3$, $Le = 1.0$, $\delta_t = \delta_c = 0.2$, Pr $= 1.0$, $\epsilon = \beta = 0.1$

Order of Approximations	$-f''(0)$	$-g''(0)$	$-\theta'(0)$	$-\phi'(0)$
1	1.13509	0.07226	0.31147	0.53000
5	1.27039	0.07329	0.35690	0.46424
10	1.33592	0.07344	0.36006	0.44888
20	1.37389	0.07360	0.36099	0.44350
25	1.38731	0.07368	0.36158	0.44215
30	1.38731	0.07368	0.36158	0.44215

4.4 Results and Discussion

This section is concerned to studied the influences of appearing parameters on respective distributions through figures $4.3 - 4.34$. Figures 4.3 and 4.4 describes $\beta' s$ (stretching rate ratio) behavior of velocity profiles. It is noticed that both velocities show conflicting behavior against $x-$ and $y-$directions for an increasing rate of β. As, $\beta = b/a$, a is smaller for higher values of β that indicates decreasing rate in velocity along $x-$axis or higher values of b specifies increasing rate along $y-$axis. Figures 4.5 and 4.6 illustrate the impacts of concentration and thermal relaxations parameters δ_c and δ_t on concentration and temperature distributions. It is noted that, both concentration and temperature fields with associated boundary layer thicknesses are decreasing functions of δ_c and δ_t respectively. Furthermore, for $\delta_t = 0$ and $\delta_c = 0$, current model will transform to classical laws of Fourier's and Fick's respectively. Figure. 4.7 describes the effect of thermal conductivity parameter ϵ on temperature profile. Higher values of ϵ provides increasing rate for the thermal boundary layer, which results in an increment in temperature distribution. Figure 4.8 exhibits the influence of Lewis number Le on concentration field. Lesser values of mass diffusivity than thermal diffusivity relative to stronger Lewis number. In result, exhausted Brownian motion coefficient bear witness to let down the nanoparticle concentration profile Figure 4.9 has drawn to depicts the impact of mixed convective parameter λ on velocity field. Higher values of λ produces stronger buoyancy force, which indicates increasing rate in the velocity field. In Figure 4.10 the effect of Prandtl number Pr on temperature profile is presented. It is to be noted that for higher values of Pr, heat diffusion from the heated surface is very slow than smaller values of Pr. Therefore, decreasing rate in temperature is preceived against

associated values of Pr. Figures 4.11 and 4.12 are drawn to illustrate the effect of Hartmann number M on both velocities profiles along $x-$ and $y-$directions. Retardation in the motion fluid is investigated due to resistance proposed by strong Lorentz force. This act finally point out decreasing rate in both velocity distributions. Figures 4.13 and 4.14 illustrates the impact of Brownian motion parameter Nb on concentration and temperature profiles. Higher values of Nb increase the temperature of the fluid in the boundary layer and instantaneously reduce particles'deposition far off from the fluid on the stretched surface. That's why temperature increases and concentration decreases. Figure 4.15 describes the effect of the thermophoresis parameter Nt on concentration field. Higher values of thermophoresis parameter Nt are in direct proportionate with temperature gradient which in turn boosts the concentration profile and its associated concentration boundary layer thickness. Figure 4.16 is drawn to depicts the effect of thermophoresis parameter Nt on temperature field. As we increase the value of Nt, movement of nanoparticles from hot to the cold ambient fluid is observed and results in higher values of temperature in the region of boundary layer. Finally, augmented thermal boundary layer thickness is identified. In Figure 4.17 the impacts of mix convective parameter λ and stretching ratio parameter β on Skin friction coefficient along $x-$direction has displayed. It is indicated that Skin friction coefficient shows increasing behaviour versus both λ and β. Similar trend can be observed in case of second grade dimensionless parameter λ and Hartmann number M against Skin friction coefficient along $x-$ direction. This impact is presented in Figure 4.18. In Figures 4.19 and 4.20, the impact of non-linear temperature's convection β_2 and non linear concentration's convection β_3 on velocity profile is displayed along $x-$ and $y-$direction. Higher values of β_2 and β_3 are in direct propotionate to velocity profile. It is to be noted that, higher values of β_2 and β_3 gives support to velocity profile, which in turn increases velocity profile. Figures 4.21 and 4.22 are drawn to display the influences of williamsons fluid parameter We on both the velocities profiles. Gradual increment in the values of We causes decrement in the values of both velocities profile. By increasing Williamsons parameter, relaxation time enhances. It causes acceleration in liquid viscosity, which results deceleration in velocity profile.Figure 4.23 illustrates the influence of Nr (ratio of concentration to thermal buoyancy forces) on velocity profile. It indicates that Nr is directly proportional to velocity profile.Therefore, acceleration in velocity profile is preceived against associated values of Nr.Figures (4.24 - 4.30) depicts

that larger values of first order slip velocity parameters (γ_1, γ_3) and magnitude of second order slip velocity parameters(γ_2, γ_4) corresponds to lower velocity. With an increasing rate in slip velocity parameters, stretching velocity is partially transferred to the fluid so velocity profiles decreases. Figure 4.31 disclose the influence of thermal stratification S_1 on $\theta(\eta)$. This figure indicates that temperature distribution is dominant for small values of S_1. It is due to potential falls between ambient temperature and surface condition. Figure 4.32 is drawn to signifies the impacts of solutal stratification S_2 on $\phi(\eta)$. Concentration identicates decaying nature with intensity of solutal stratification. In fact, reduction in concentration difference between ambient fluid and the sheet is detected, which finally declines the concentration field. Figure 4.33 is drawn to understand the impact of We (Williamsons parameter) and β_3(non-linear concentration's convection) on the skin friction coefficient along $x-$direction. It in indicated that skin friction displays increasing behaviour versus both We and β_3. Analysis of the influence of λ and Nr on skin friction is discribed in Fig. 4.34. It is to be noted that thinner boundary layer is associated with larger λ,which result in higher velocity gradient near the wall. That's why skin friction reduces against λ.

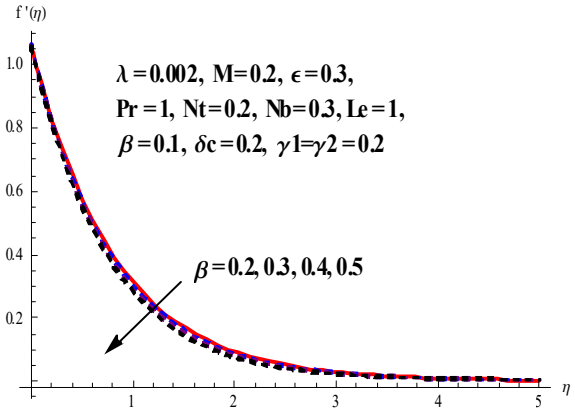

Fig 4.3. Impact of β on f'

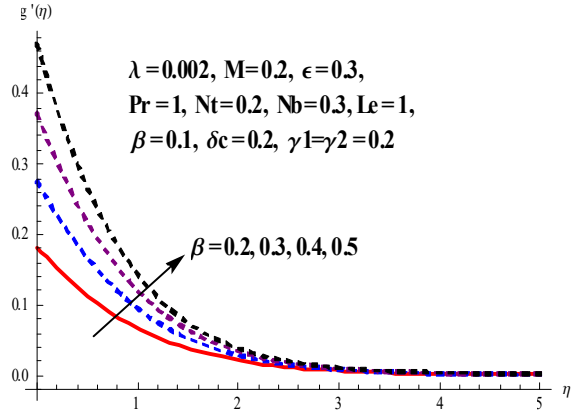

Fig 4.4. Impact of β on g'

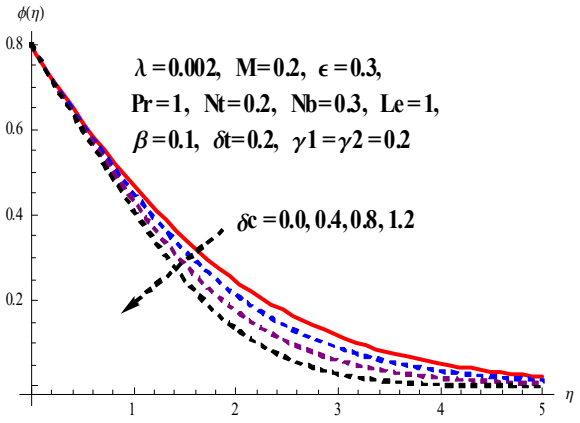

Fig 4.5. Impact of δ_c on ϕ

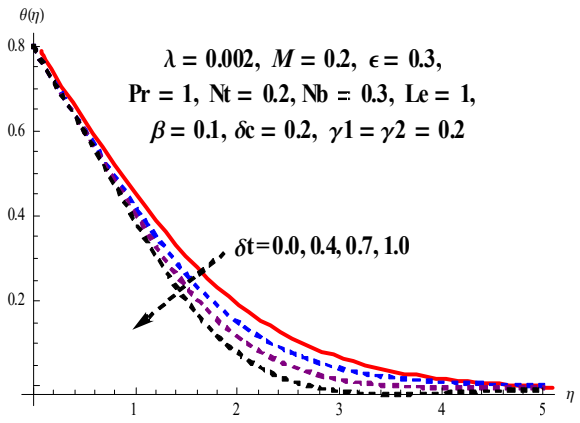

Fig 4.6. Impact of δ_t on θ

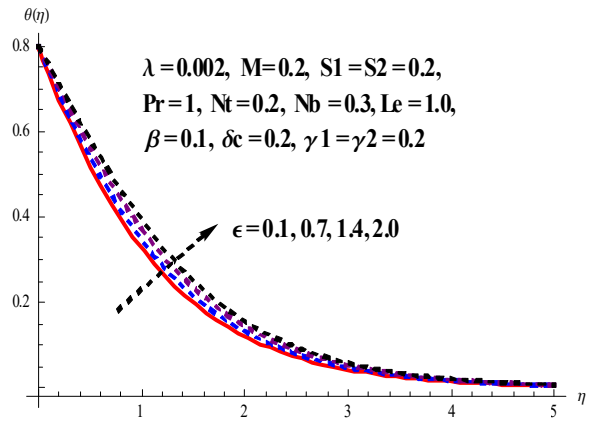

Fig 4.7. Impact of ϵ on θ

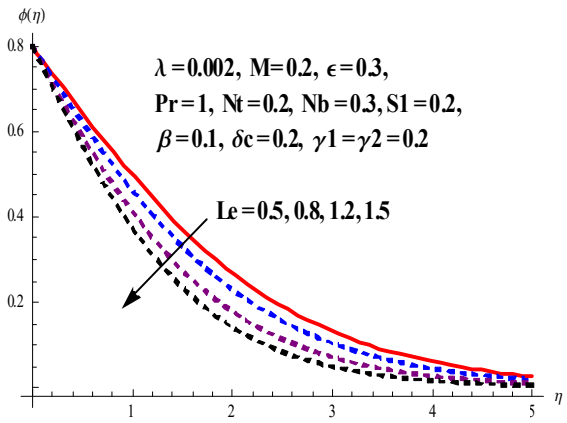

Fig 4.8. Impact of Le on ϕ

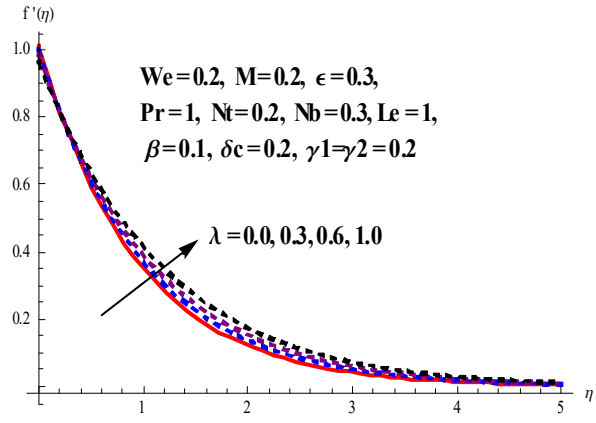

Fig 4.9. Impact of λ on f'

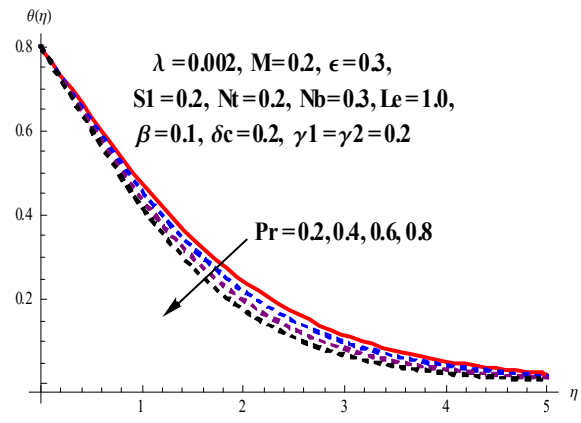

Fig 4.10. Impact of Pr on θ

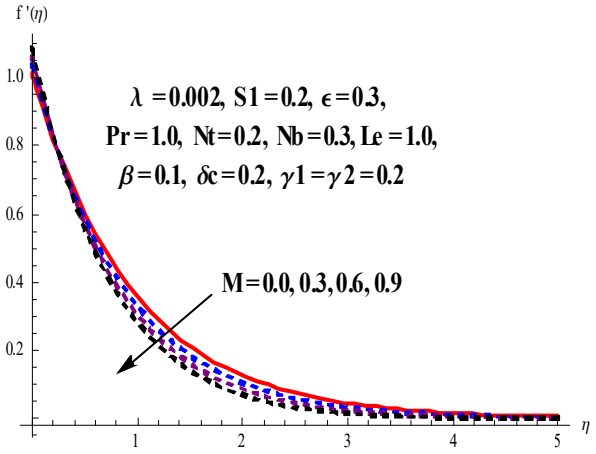

Fig 4.11. Impact of M on f'

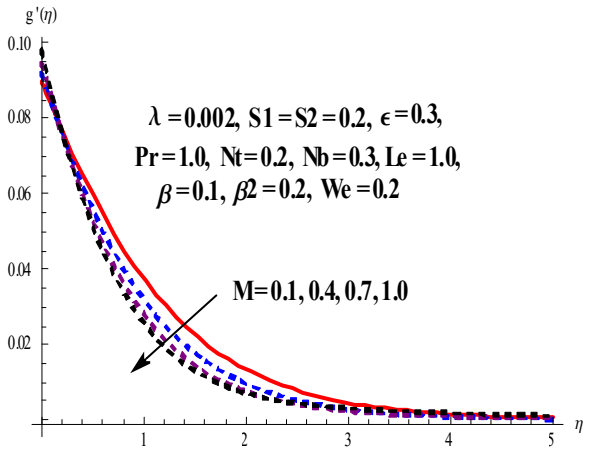

Fig 4.12. Impact of M on g'

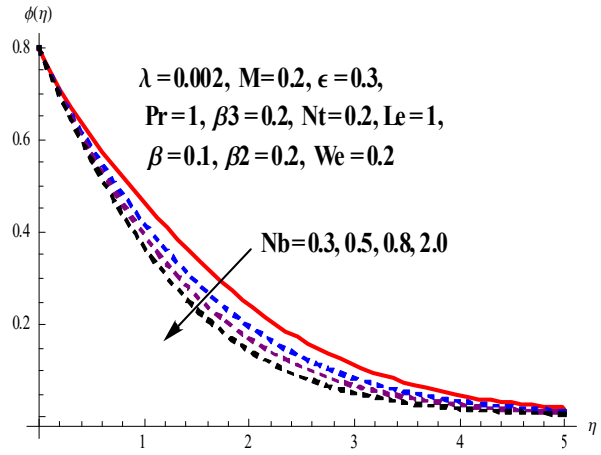

Fig 4.13. Impact of Nb on ϕ

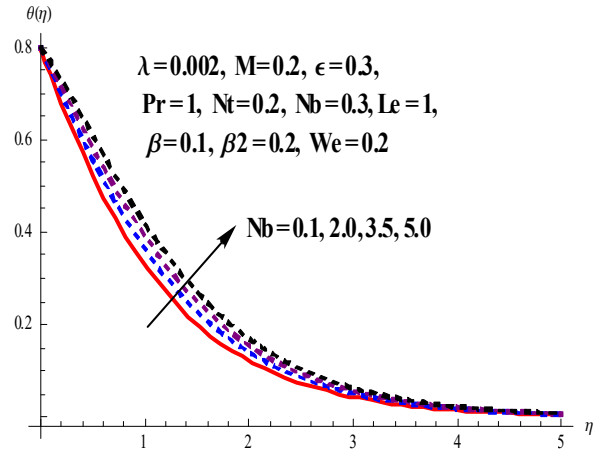

Fig 4.14. Impact of Nb on θ

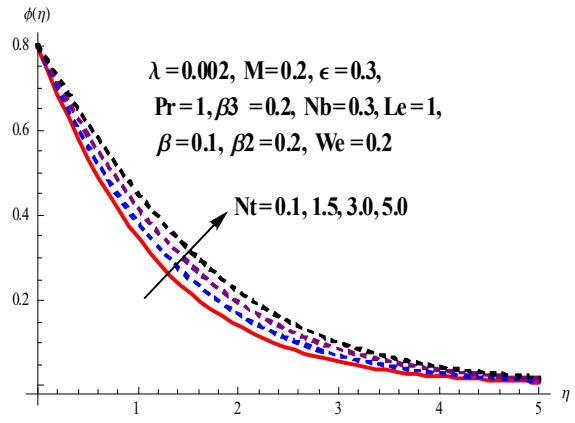

Fig 4.15. Impact of Nt on ϕ

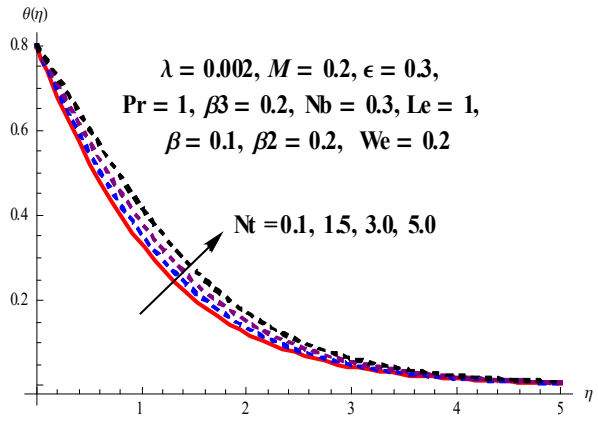

Fig 4.16. Impact of Nt on θ

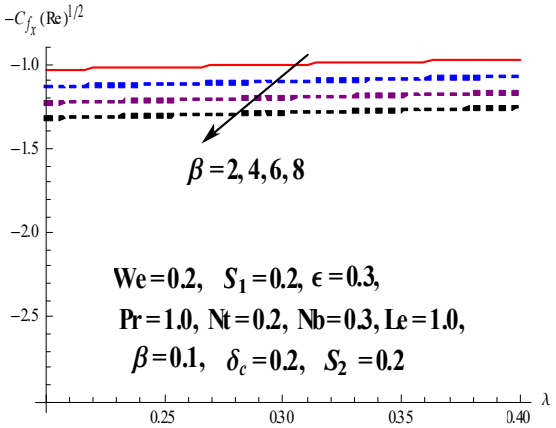

Fig. 4.17 Impact of λ and β on $C_{f_x}(\mathrm{Re})^{1/2}$

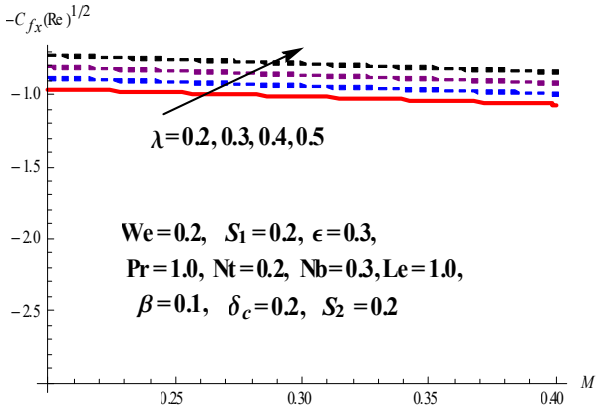

Fig. 4.18 Impact of λ and M on $C_{f_x}(\mathrm{Re})^{1/2}$

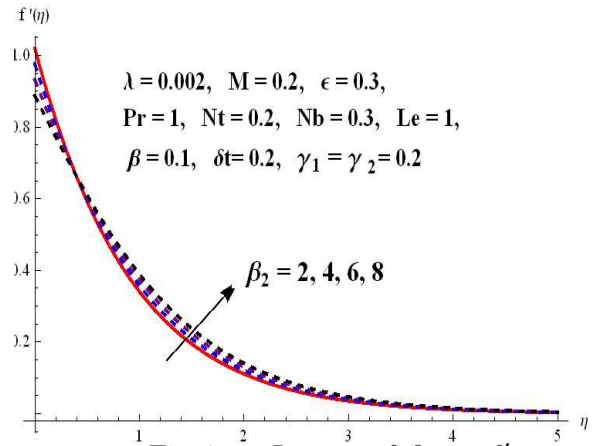

Fig 4.19. Impact of β_2 on f'

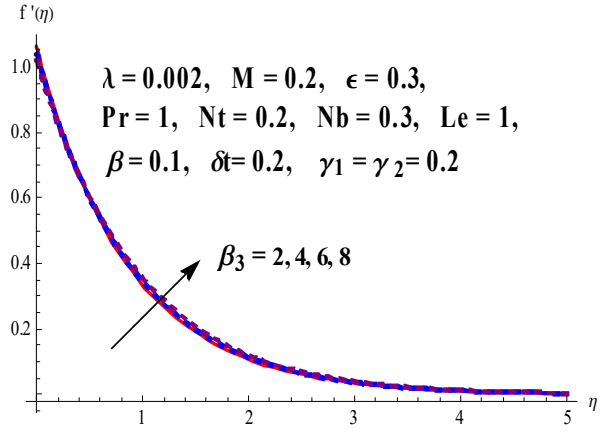

Fig 4.20. Impact of β_3 on f'

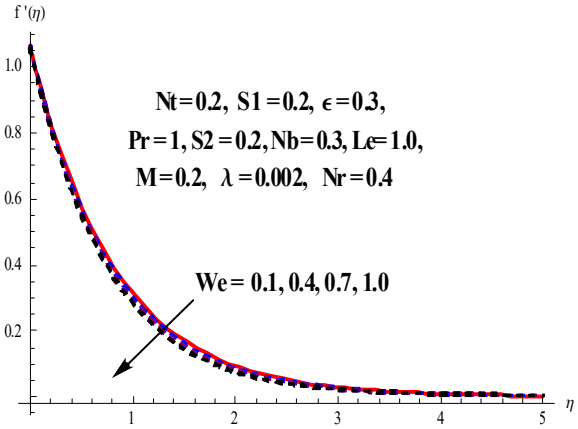

Fig 4.21. Impact of We on f'

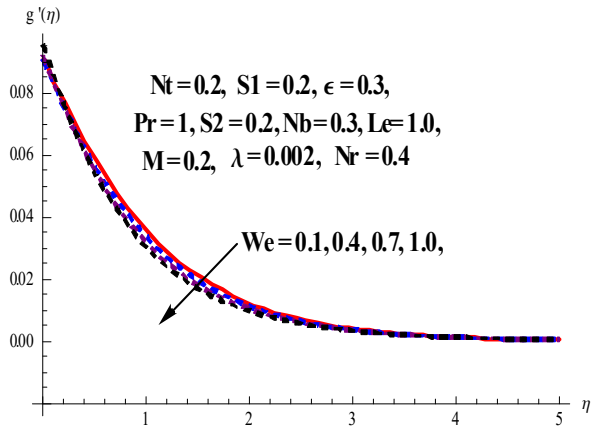

Fig 4.22. Impact of We on g'

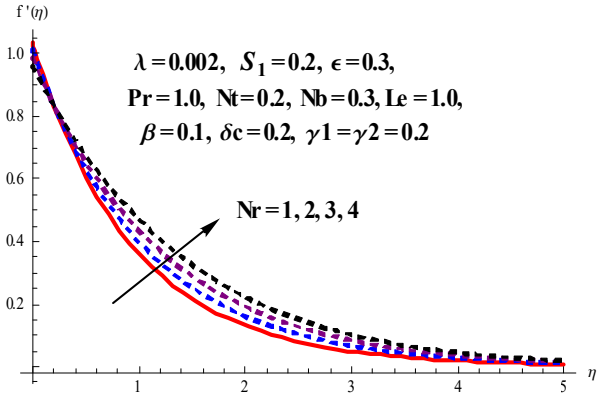

Fig. 4.23. Impact of Nr on f'

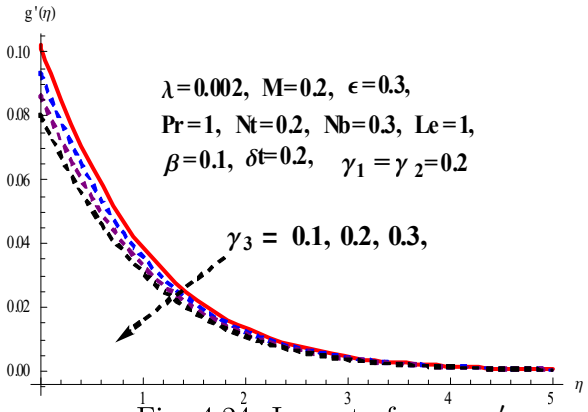

Fig. 4.24. Impact of γ_3 on g'

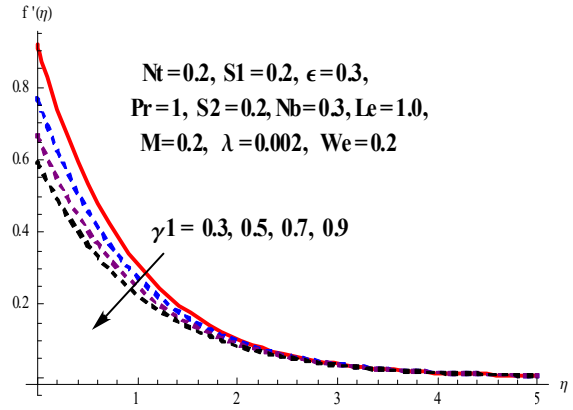

Fig 4.25. Impact of γ_1 on f'

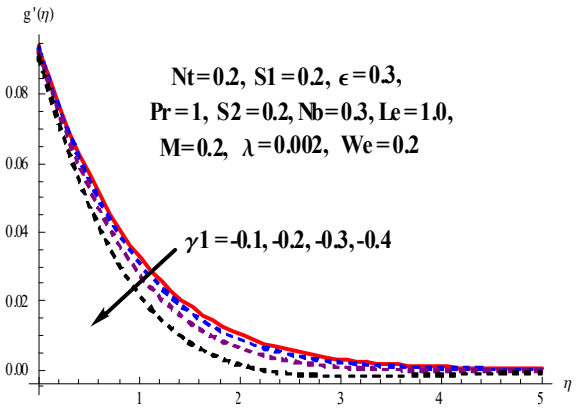

Fig 4.26. Impact of γ_1 on g'

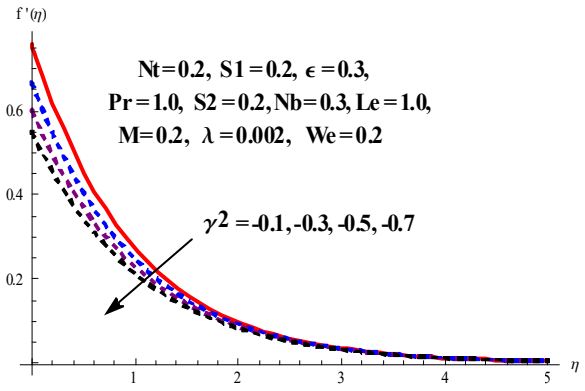

Fig 4.27. Impact of γ_2 on f'

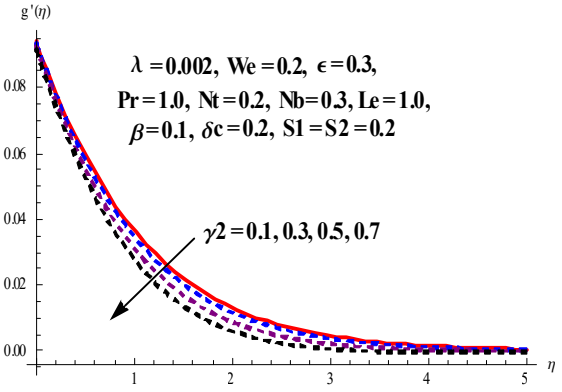

Fig 4.28. Impact of γ_2 on g'

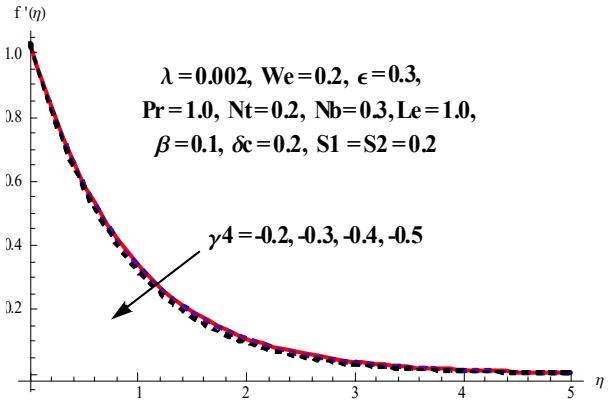

Fig 4.29. Impact of γ_4 on f'

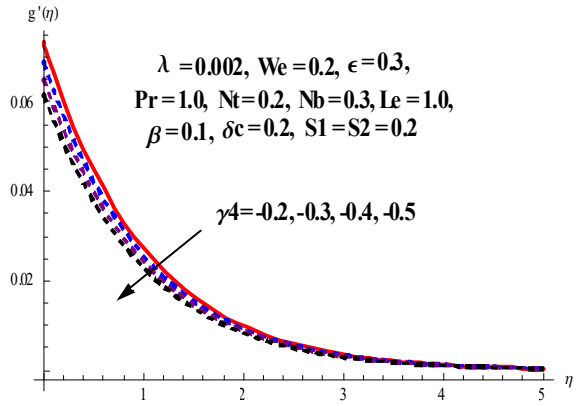

Fig 4.30. Impact of γ_4 on g'

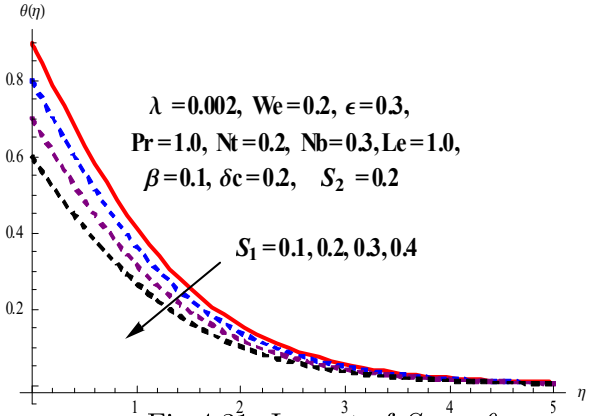

Fig 4.31. Impact of S_1 on θ

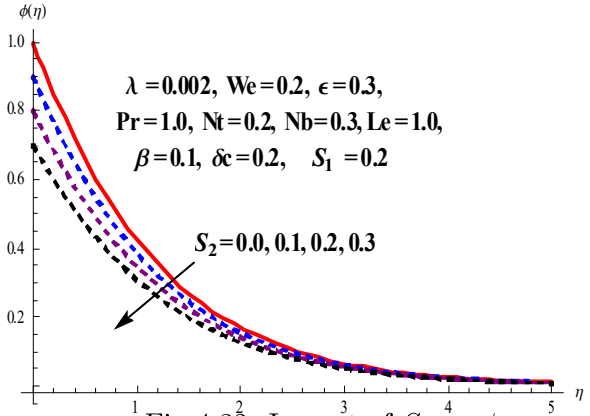

Fig 4.32. Impact of S_2 on ϕ

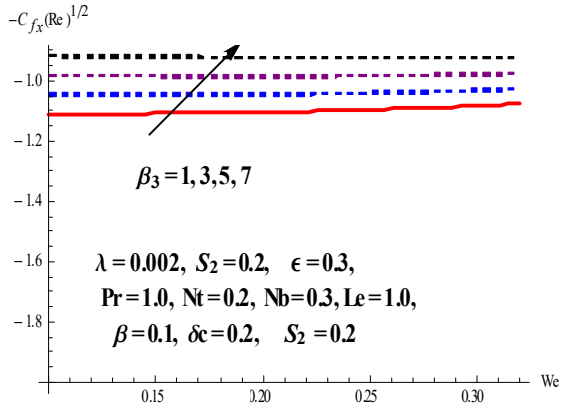

Fig. 4.33. Impact of β_3 and We on $C_{fx}(\mathrm{Re})^{1/2}$

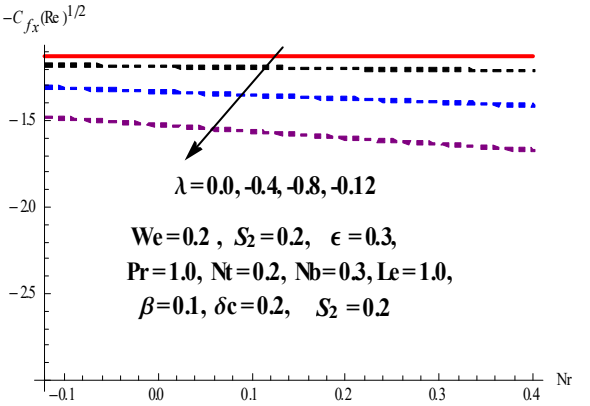

Fig. 4.34. Impact of Nr and λ on $C_{fx}(\mathrm{Re})^{1/2}$

Chapter 5

Concluding Remarks and Future work

In this thesis, two problems have been analysed where first problem is about review paper and second problem is the extension work for it. Conclusion of both problems are as following:

5.1 Chapter 3 (conclusion)

In this study, we have investigated the flow of second grade nanofluid flow past a bidirectional stretched surface in the presence of magneto hydrodynamic, generalized Fourier's and Fick's laws, and variable thermal conductivity. Analysis is performed under the influence of convective heat and mass boundary conditions. Analytic results in the form of series solutions are found via Homotopy Analysis method (HAM). Significant findings of the investigation are as follows:

- Velocities along $x-$ and $y-$directions exhibit conflicting trend against stretching ratio parameter.
- Thermal and concentration relaxations parameters show decreasing behavior on temperature and concentration distributions respectively.
- Higher values of thermal conductivity parameter lead to increased temperature.
- Brownian motion and thermophoresis parameters have contrary behavior on concentration

field.

- Skin friction coefficient along $y-$direction is enhanced for increasing values of second grade parameter and Hartman number.

5.2 Chapter 4 (conclusion)

In this study, we have investigated the flow Williamsons nanofluid past a bidirectional stretched surface in the presence of magneto hydrodynamic and generalized Fourier's and Fick's laws,. Analysis is performed under the influence of second order slip and double stratification. Analytic results in the form of series solutions are found via Homotopy Analysis method (HAM). Significant findings of the investigation are as follows:

- Velocities along $x-$ and $y-$directions exhibit conflicting trend against Williamsons fluid parameter.
- Thermal and concentration stratification parameters show decreasing behavior on temperature and concentration distributions respectively.
- Higher values of mixed convection parameter lead to increased velocity profile along $x-$direction.
- Higher values of non-linear temperature convection and non-linear concentration convection parameter lead to increased velocity profile along $x-$direction
- Brownian motion and thermophoresis parameters have contrary behavior on concentration field.
- Skin friction coefficient along $x-$direction shows decreasing behaviour for increasing values of Williamsons fluid parameter and non-linear concentration convection parameter.

5.3 Future work

Few interesting possible problems that could be researched in future are as follows:

- The proposed model may be extended to some other non-Newtonian fluid.

- The impact of buoyancy effect and Darcy-Forchheimer may be added to the momentum equation.
- The energy equation may be enhanced by adding the impact of Joule heating and viscous dissipation.
- The model presented here may be extended for homogeneous-heterogeneous reactions.
- The concentration equation can be inforced by chemical reaction and Arrhenis activation energy.
- The boundary conditions may be replaced by convective heat and mass and melting heat.
- The geometry of the problem may be changed to a cylinder, rotating disk or fluid may be taken in a channel.

Bibliography

[1] Straughan, B. (2010). Thermal convection with the Cattaneo–Christov model. International Journal of Heat and Mass Transfer, 53(1-3), 95-98.

[2] Khan, W. A., Khan, M., Alshomrani, A. S., & Ahmad, L. (2016). Numerical investigation of generalized Fourier's and Fick's laws for Sisko fluid flow. Journal of Molecular Liquids, 224, 1016-1021.

[3] Hayat, T., Khan, M. I., Farooq, M., Alsaedi, A., Waqas, M., & Yasmeen, T. (2016). Impact of Cattaneo–Christov heat flux model in flow of variable thermal conductivity fluid over a variable thicked surface. International Journal of Heat and Mass Transfer, 99, 702-710.

[4] Waqas, M., Hayat, T., Farooq, M., Shehzad, S. A., & Alsaedi, A. (2016). Cattaneo-Christov heat flux model for flow of variable thermal conductivity generalized Burgers fluid. Journal of Molecular Liquids, 220, 642-648.

[5] Khan, U., Ahmed, N., & Mohyud-Din, S. T. (2016). Thermo-diffusion and diffusion-thermo effects on flow of second grade fluid between two inclined plane walls. Journal of Molecular Liquids, 224, 1074-1082.

[6] Ghadikolaei, S. S., Hosseinzadeh, K., Yassari, M., Sadeghi, H., & Ganji, D. D. (2018). Analytical and numerical solution of non-Newtonian second-grade fluid flow on a stretching sheet. Thermal Science and Engineering Progress, 5, 309-316.

[7] Khan, I., Malik, M. Y., Salahuddin, T., Khan, M., & Rehman, K. U. (2018). Homogenous–heterogeneous reactions in MHD flow of Powell–Eyring fluid over a stretching sheet with Newtonian heating. Neural Computing and Applications, 30(11), 3581-3588.

[8] Ibrahim, W., Shankar, B., & Nandeppanavar, M. M. (2013). MHD stagnation point flow and heat transfer due to nanofluid towards a stretching sheet. International Journal of Heat and Mass Transfer, 56(1-2), 1-9.

[9] Chamkha, A. J., & Al-Mudhaf, A. (2005). Unsteady heat and mass transfer from a rotating vertical cone with a magnetic field and heat generation or absorption effects. International journal of thermal sciences, 44(3), 267-276.

[10] Pullepu, B., Chamkha, A. J., & Pop, I. (2012). Unsteady laminar free convection flow past a non-isothermal vertical cone in the presence of a magnetic field. Chemical Engineering Communications, 199(3), 354-367.

[11] Akbar, N. S., Nadeem, S., Haq, R. U., & Khan, Z. H. (2013). Numerical solutions of Magnetohydrodynamic boundary layer flow of tangent hyperbolic fluid towards a stretching sheet. Indian journal of Physics, 87(11), 1121-1124.

[12] Seini, I.Y. and Makinde, O.D. (2014). Boundary layer flow near stagnation-points on a verticalsurface with slip in the presence of transverse magnetic field. International Journal of Numerical Methods for Heat and Fluid Flow, 24(3), 643-653.

[13] Ravindran, R., Ganapathirao, M., & Pop, I. (2014). Effects of chemical reaction and heat generation/absorption on unsteady mixed convection MHD flow over a vertical cone with non-uniform slot mass transfer. International Journal of Heat and Mass Transfer, 73, 743-751.

[14] Bovand, M., Rashidi, S., Esfahani, J. A., Saha, S. C., Gu, Y. T., & Dehesht, M. (2016). Control of flow around a circular cylinder wrapped with a porous layer by magnetohydrodynamic. Journal of Magnetism and Magnetic Materials, 401, 1078-1087.

[15] Ellahi, R., Bhatti, M. M., & Pop, I. (2016). Effects of hall and ion slip on MHD peristaltic flow of Jeffrey fluid in a non-uniform rectangular duct. International Journal of Numerical Methods for Heat & Fluid Flow, 26(6), 1802-1820.

[16] Mishra, S. R., Pattnaik, P. K., Bhatti, M. M., & Abbas, T. (2017). Analysis of heat and mass transfer with MHD and chemical reaction effects on viscoelastic fluid over a stretching sheet. Indian Journal of Physics, 91(10), 1219-1227.

[17] Hussain, A., Malik, M. Y., Awais, M., Salahuddin, T., & Bilal, S. (2019). Computational and physical aspects of MHD Prandtl-Eyring fluid flow analysis over a stretching sheet. Neural Computing and Applications, 31(1), 425-433.

[18] Khan, W. A., & Pop, I. (2010). Boundary-layer flow of a nanofluid past a stretching sheet. International journal of heat and mass transfer, 53(11-12), 2477-2483.

[19] Makinde, O. D., & Aziz, A. (2011). Boundary layer flow of a nanofluid past a stretching sheet with a convective boundary condition. International Journal of Thermal Sciences, 50(7), 1326-1332.

[20] Nadeem, S., Mehmood, R., & Akbar, N. S. (2013). Non-orthogonal stagnation point flow of a nano non-Newtonian fluid towards a stretching surface with heat transfer. International Journal of Heat and Mass Transfer, 57(2), 679-689.

[21] Hatami, M., Jing, D., Song, D., Sheikholeslami, M., & Ganji, D. D. (2015). Heat transfer and flow analysis of nanofluid flow between parallel plates in presence of variable magnetic field using HPM. Journal of Magnetism and Magnetic Materials, 396, 275-282.

[22] Hayat, T., Imtiaz, M., & Alsaedi, A. (2015). MHD 3D flow of nanofluid in presence of convective conditions. Journal of Molecular Liquids, 212, 203-208.

[23] Sheikholeslami, M., Ganji, D. D., Javed, M. Y., & Ellahi, R. (2015). Effect of thermal radiation on magnetohydrodynamics nanofluid flow and heat transfer by means of two phase model. Journal of Magnetism and Magnetic Materials, 374, 36-43.

[24] Sheikholeslami, M., & Rokni, H. B. (2017). Nanofluid two phase model analysis in existence of induced magnetic field. International Journal of Heat and Mass Transfer, 107, 288-299.

[25] Hassan, M., Marin, M., Alsharif, A., & Ellahi, R. (2018). Convective heat transfer flow of nanofluid in a porous medium over wavy surface. Physics Letters A, 382(38), 2749-2753.

[26] Nayak, M. K., Shaw, S., Pandey, V. S., & Chamkha, A. J. (2018). Combined effects of slip and convective boundary condition on MHD 3D stretched flow of nanofluid through porous media inspired by non-linear thermal radiation. Indian Journal of Physics, 1-12

[27] Hosseini, S. R., Sheikholeslami, M., Ghasemian, M., & Ganji, D. D. (2018). Nanofluid heat transfer analysis in a microchannel heat sink (MCHS) under the effect of magnetic field by means of KKL model. Powder Technology, 324, 36-47.

[28] Lu, D., Ramzan, M., Mohammad, M., Howari, F., & Chung, J. D. (2019). A Thin Film Flow of Nanofluid Comprising Carbon Nanotubes Influenced by Cattaneo-Christov Heat Flux and Entropy Generation. Coatings, 9(5), 296.

[29] Li, Z., Shafee, A., Ramzan, M., Rokni, H. B., & Al-Mdallal, Q. M. (2019). Simulation of natural convection of Fe 3 O 4-water ferrofluid in a circular porous cavity in the presence of a magnetic field. The European Physical Journal Plus, 134(2), 77.

[30] Suleman, M., Ramzan, M., Ahmad, S., Lu, D., Muhammad, T., & Chung, J. D. (2019). A Numerical Simulation of Silver–Water Nanofluid Flow with Impacts of Newtonian Heating and Homogeneous–Heterogeneous Reactions Past a Nonlinear Stretched Cylinder. Symmetry, 11(2), 295.

[31] Lu, D., Li, Z., Ramzan, M., Shafee, A., & Chung, J. D. (2019). Unsteady squeezing carbon nanotubes based nano-liquid flow with Cattaneo–Christov heat flux and homogeneous–heterogeneous reactions. Applied Nanoscience, 9(2), 169-178.

[32] Ramzan, M., Sheikholeslami, M., Saeed, M., & Chung, J. D. (2019). On the convective heat and zero nanoparticle mass flux conditions in the flow of 3D MHD Couple Stress nanofluid over an exponentially stretched surface. Scientific reports, 9(1), 562.

[33] Li, Z., Sheikholeslami, M., Shafee, A., Ramzan, M., Kandasamy, R., & Al-Mdallal, Q. M. (2019). Influence of adding nanoparticles on solidification in a heat storage system considering radiation effect. Journal of Molecular Liquids, 273, 589-605.

[34] Farooq, U., Lu, D. C., Munir, S., Suleman, M., & Ramzan, M. (2019). Flow of Rheological Nanofluid Over a Static Wedge. Journal of Nanofluids, 8(6), 1362-1366.

[35] S. J. Liao, Beyond Perturbation (Chapman & Hall/CRC Press, Boca Raton, 2003).

[36] K. Ahmad, R. Nazar, Magnetohydrodynamic threedimensional flow and heat transfer over a stretching surface in a viscoelastic fluid, Journal of Science and Technology, 3 (1) (2011).